Allosteric Activation of Cytochrome P450 3A4 via Progesterone Bioconjugation

Vanja Polic, and Karine Auclair

Department of Chemistry, McGill University, 801 Sherbrooke Street West, Montreal, Quebec, Canada H3A 0B8

1. SUPPORTING FIGURES

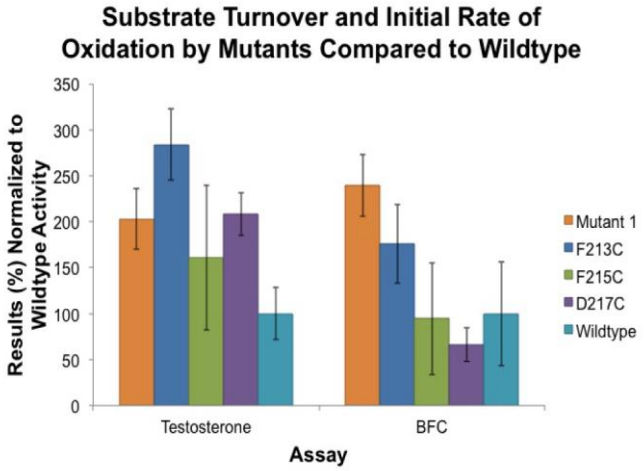

Figure S1. Transformation of testosterone and BFC by CYP3A4 cysteine mutants before bioconjugation, compared wildtype CYP3A4.
Total turnover and initial rate of oxidation by CYP3A4 cysteine mutants (without bioconjugation) were measured with two assays and compared to those of wildtype CYP3A4. 1) The total turnover of testosterone was measured after 1 hour as detailed in Section 2.7. The testosterone assay consisted of 0.4 µM CYP3A4, 600 µM CHP, and 115 µM testosterone in a 150 µL volume. 2) Initial rate of catalysis was determined using 7-benzyloxy-(4-trifluoromethyl)coumarin (BFC) transformation as detailed in Sections 2.6.. The BFC assay consisted of 0.4 µM CYP3A4, 1.6 µM CPR, 33 µM BFC and 1 mM NADPH in a 150 µL volume. Initial rate was determined from the linear segment at the beginning of the kinetic curve. The data is shown as an average from duplicates or triplicates, and normalized to wildtype enzyme (100%). The error bars show standard deviation, and outliers were removed as determined by the Tukey method.[1]

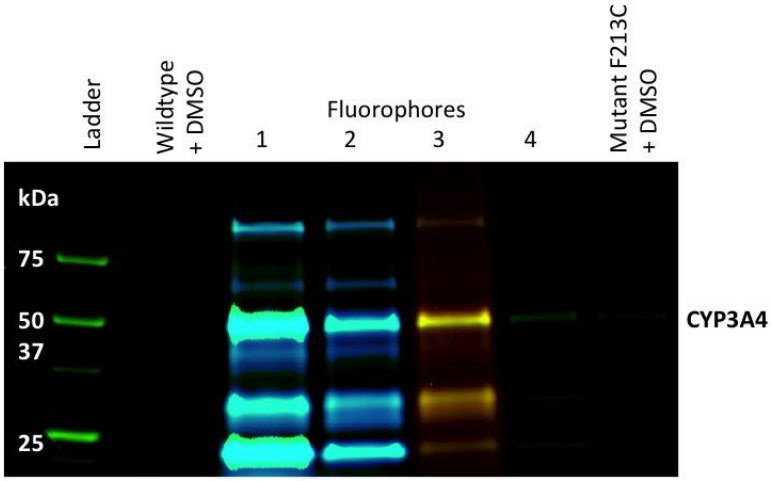

Figure S2. SDS-PAGE of Mutant F213C conjugated to fluorophores

Conjugation results for mutant F213C. Blue bands correspond to blue epi transillumination with an emission cutoff at 530 nm for visualizing AlexaFluor 488 and fluorescein, orange/yellow bands to green epi transillumination with an emission cutoff at 605 nm for visualizing DyLight550, green bands to unlabeled proteins or proteins labeled with coumarin. The major band at ~ 50 kDa corresponds to fluorophore-labeled CYP3A4. Other major bands around ~25 and 30 kDa are likely fluorophore-labeled degradation products of CYP3A4. The less fluorescent bands correspond to other cysteine-containing proteins that co-eluted with CYP3A4 during purification and proceeded to be labeled by the maleimide-containing fluorophores. Evidence of CYP3A4 labeling by coumarin is shown by comparing lane 4 (coumarin labeled protein) with the Mutant F215C+DMSO control (non-labeled protein). The presence of conjugated coumarin produces a stronger signal when illuminated by UV than non-labeled protein control.

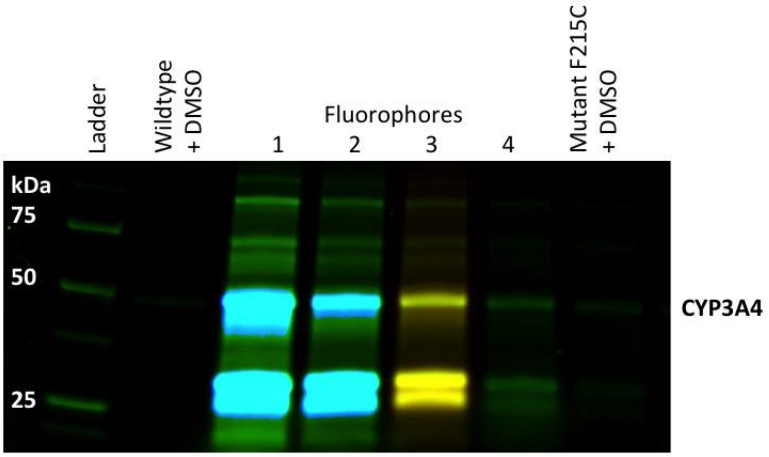

Figure S3. SDS-PAGE of Mutant F215C conjugated to fluorophores
Conjugation results for mutant F215C. Blue bands correspond to blue epi transillumination with an emission cutoff at 530 nm for visualizing AlexaFluor 488 and fluorescein, orange/yellow bands to green epi transillumination with an emission cutoff at 605 nm for visualizing DyLight550, green bands to unlabeled proteins or proteins labeled with coumarin. The major band at ~ 50 kDa corresponds to fluorophore-labeled CYP3A4. Other major bands around ~25 and 30 kDa are likely fluorophore-labeled degradation products of CYP3A4. The less fluorescent bands correspond to other cysteine-containing proteins that co-eluted with CYP3A4 during purification and proceeded to be labeled by the maleimide-containing fluorophores. Evidence of CYP3A4 labeling by coumarin is shown by comparing lane 4 (coumarin labeled protein) with the Mutant F215C+DMSO control (non-labeled protein). The presence of conjugated coumarin produces a stronger signal when illuminated by UV than non-labeled protein control.

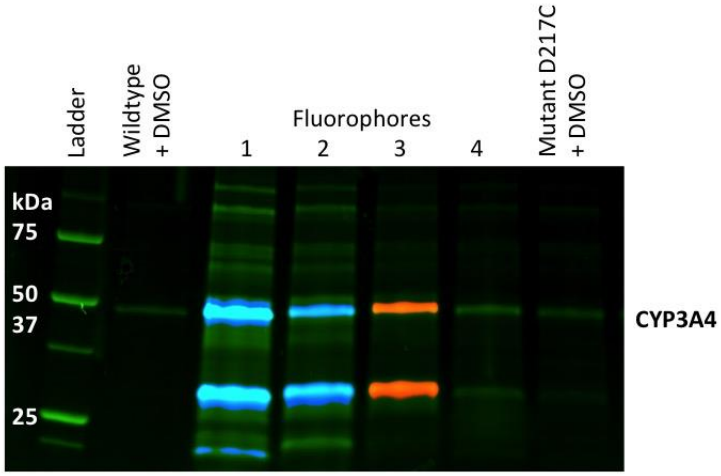

Figure S4. SDS-PAGE of Mutant D217C conjugated to fluorophores
Conjugation results for mutant D217C. Blue bands correspond to blue epi transillumination with an emission cutoff at 530 nm for visualizing AlexaFluor 488 and fluorescein, orange/yellow bands to green epi transillumination with an emission cutoff at 605 nm for visualizing DyLight550, green bands to unlabeled proteins or proteins labeled with coumarin. The major band at ~ 50 kDa corresponds to fluorophore-labeled CYP3A4. Other major band at ~ 30 kDa is likely a fluorophore-labeled degradation product of CYP3A4. The less fluorescent bands correspond to other cysteine-containing proteins that co-eluted with CYP3A4 during purification and proceeded to be labeled by the maleimide-containing fluorophores. Evidence of CYP3A4 labeling by coumarin is shown by comparing lane 4 (coumarin labeled protein) with the Mutant D217C+DMSO control (non-labeled protein). The presence of conjugated coumarin produces a stronger signal when illuminated by UV than non-labeled protein control.

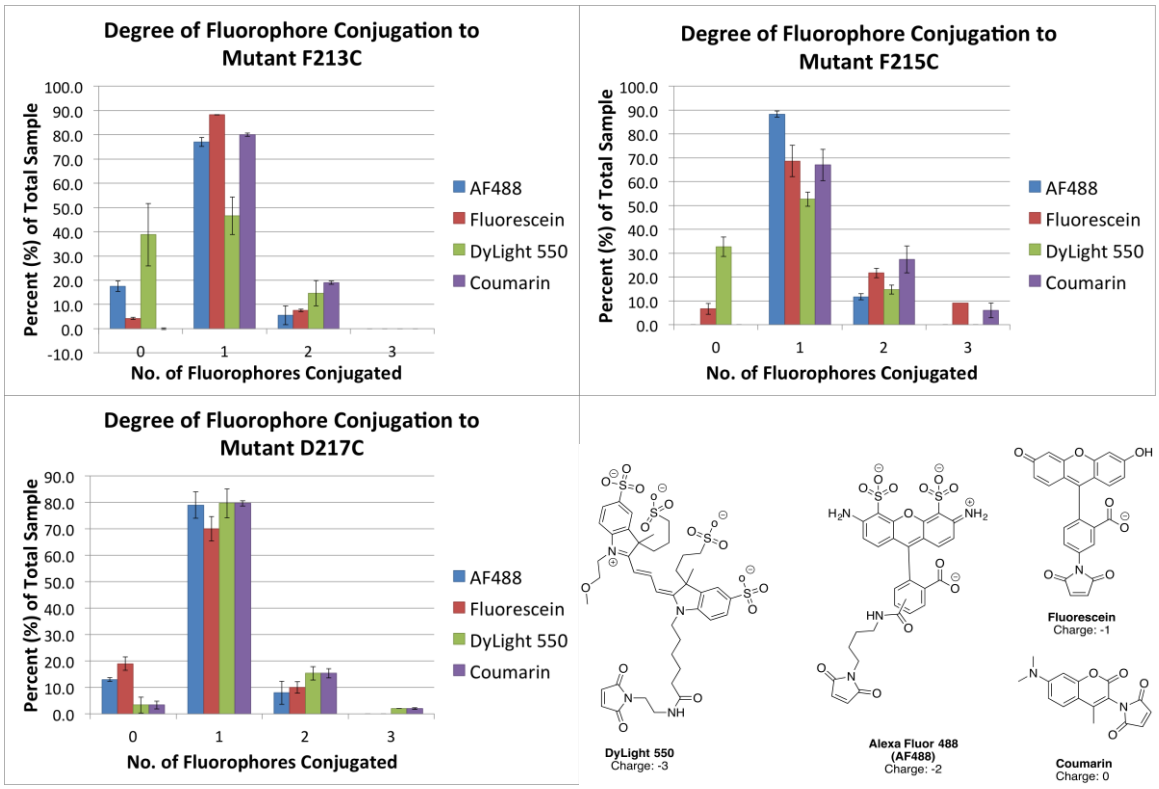

	Degree (%) of Labeling of Total CYP3A4											
Mutant →	**F213C**				**F215C**				**D217C**			
No. of Labels →	**0**	**1**	**2**	**3**	**0**	**1**	**2**	**3**	**0**	**1**	**2**	**3**
Alexa Fluor 488	17.5	77.0	5.5	0.0	13.0	79.0	8.0	0.0	0.0	88.3	11.7	0.0
Fluorescein	4.3	88.2	7.5	0.0	19.0	70.0	10.0	0.0	6.7	68.7	21.7	9.0
DyLight 550	38.8	46.6	14.6	0.0	37.0	53.0	9.0	0.0	32.7	52.7	14.7	0.0
Coumarin	0.0	80.0	19.0	0.0	3.3	79.7	15.3	2.0	0.0	67.0	27.3	6.0

Figure S5. Degree of CYP3A4 cysteine mutant labeling by fluorophores
The degree of labeling was obtained from the QTOF-MS spectra (See section S5). Percent labeling was calculated by dividing the area under each peak corresponding to mutant CYP3A4 by the sum of the areas under all the peaks corresponding to CYP3A4. The percentage of each labeled species is reported in the table. A visual representation showing the trend relating to molecular structure is shown in the graphs. No distinction is made between active or inactive CYP3A4, with the inactive CYP3A4 being double or triple labeled. Each sample is an average of three experiments with the standard deviation shown as error bars in the graphs.

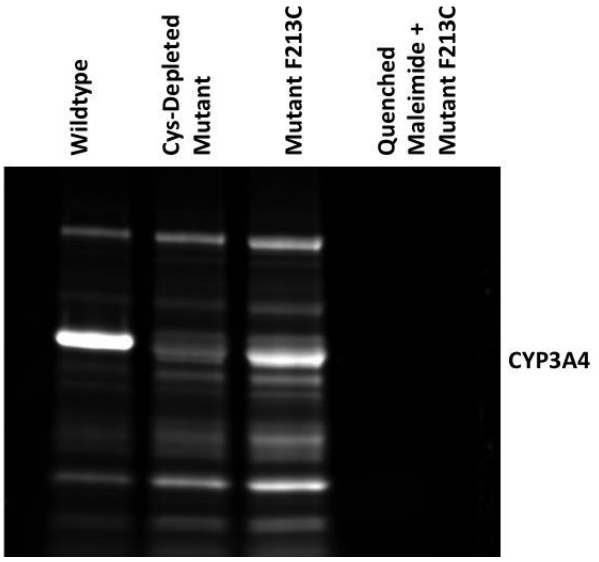

Figure S6. Comparison of CYP3A4 mutants with varying amounts cysteines by fluorophore conjugation

The above gel compares the relative labeling of CYP3A4 variants with different number of cysteines present, as well as the degree of labeling by maleimide-containing fluorophore quenched with DTT. The numbers of cysteines present are as follows: wildtype has 7, Cys-depleted mutant has 2, and mutant F213C has 3. With more cysteines present, the fluorescent signal for the CYP3A4 band is stronger while with the quenched maleimide control, no labeling of the protein occurred. The presence of other fluorescently labeled bands suggests both degradation of the protein as well as the presence of other cysteine-containing protein that co-eluted with CYP3A4 during purification.

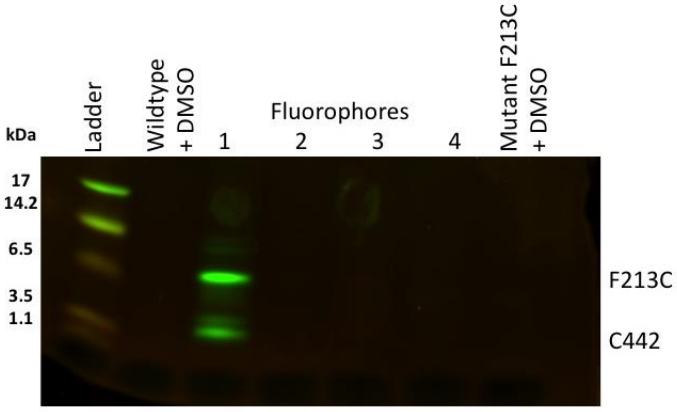

Figure S7. Tricine-SDS-PAGE of Mutant F213C.

The major bands above 6.5 and 3.5 kDa correspond to fluorophore-labeled peptides fragments containing C213 and C442 expected at ~ 8.6 and 5.9 kDa respectively. The final peptide fragment containing the third cysteine that was not labeled is expected at 1.7 kDa. Green bands correspond to blue epi transillumination with an emission cutoff at 530

nm for visualizing AlexaFluor 488, and molecular weight markers. After staining of the tricine gels with SyproOrange fluorophores 2, 3 and 4 are not visible due to fluorescence quenching.

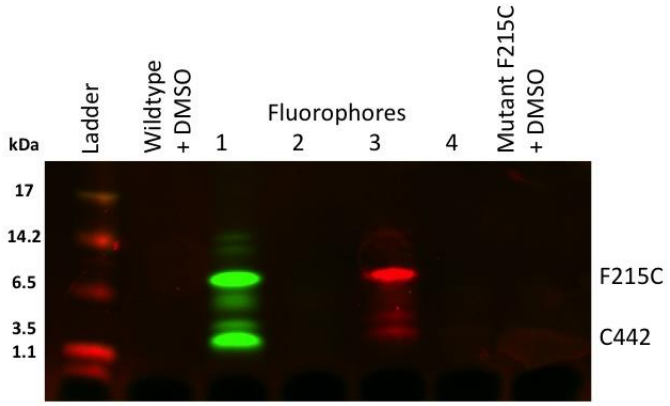

Figure S8. Tricine-SDS-PAGE of Mutant F215C.
The major bands above 6.5 and 3.5 kDa correspond to fluorophore-labeled peptides fragments containing C215 and C442 expected at ~ 8.6 and 5.9 kDa respectively. The final peptide fragment containing the third cysteine that was not labeled is expected at 1.7 kDa. Green bands correspond to blue epi transillumination with an emission cutoff at 530 nm for visualizing AlexaFluor 488, red bands to green epi transillumination with an emission cutoff at 605 nm for visualizing DyLight550, and molecular weight markers are shown in red. After staining of the tricine gels with SyproOrange fluorophores 2, and 4 are not visible due to fluorescence quenching.

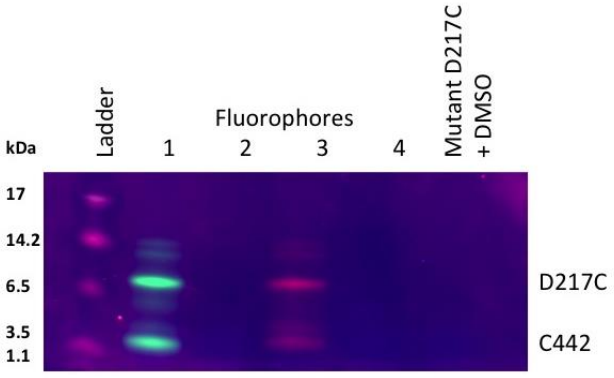

Figure S9. Tricine-SDS-PAGE of Mutant D217C.
The major bands above 6.5 and 3.5 kDa correspond to fluorophore-labeled peptides fragments containing C217 and C442 expected at ~ 8.6 and 5.9 kDa respectively. The final peptide fragment containing the third cysteine that was not labeled is expected at 1.7 kDa. Green bands correspond to blue epi transillumination with an emission cutoff at 530 nm for visualizing AlexaFluor 488, red bands to green epi transillumination with an emission cutoff at 605 nm for visualizing DyLight550, and molecular weight markers are shown in red. After staining of the tricine gels with SyproOrange fluorophores 2, and 4 are not visible due to fluorescence quenching.

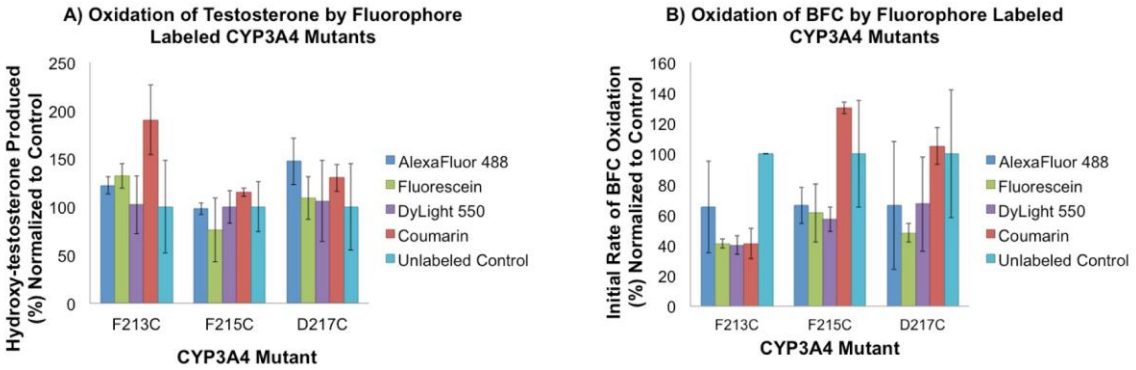

Figure S10. Effect of conjugated fluorophores of mutant CYP3A4 on testosterone turnover and initial rate of BFC transformation.
A) Effect of conjugated fluorophores on the hydroxylation of testosterone by each CYP3A4 mutant. The reaction was performed as described in section 2.7 below and consisted of 0.4 µM CYP3A4, 600 µM CHP, and 115 µM testosterone in a 150 µL volume. B) Effect of conjugated fluorophores on the enzymatic transformation of BFC by each CYP3A4 mutant. The reaction was performed as described in Section 2.6 below and consisted of 0.4 µM CYP3A4, 1.6 µM CPR, 33 µM BFC and 1 mM NADPH in a 150 µL volume. Activity data for each mutant is normalized to its own unlabeled control, which was treated identically to the maleimide-ligand containing reactions but lacked a ligand. Each data point is the average of three experiments with standard deviation shown by the error bars.

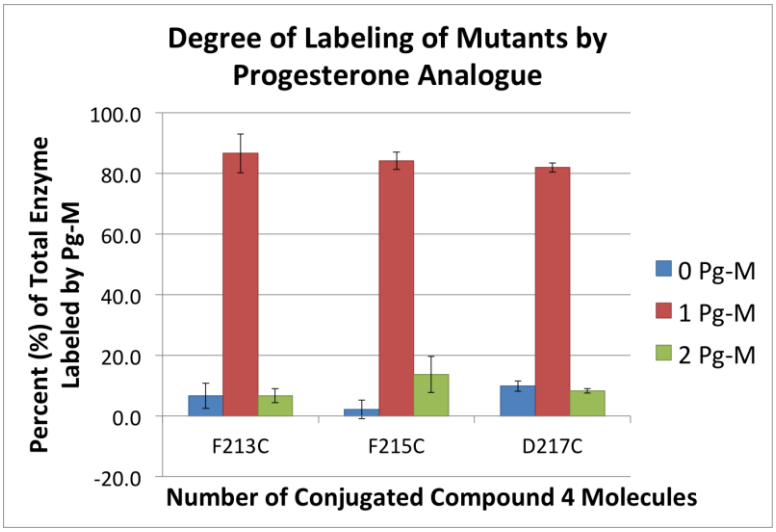

	Degree (%) of Labeling of Total CYP3A4											
Mutant →	**F213C**				**F215C**				**D217C**			
No. of Labels →	**0**	**1**	**2**	**3**	**0**	**1**	**2**	**3**	**0**	**1**	**2**	**3**
Pg-M	6.7	86.7	6.7	0.0	2.2	84.3	13.6	0.0	9.8	82.0	8.2	0.0

Figure S11. Degree of CYP3A4 labeling by progesterone-maleimide (Pg-M)
The degree of CYP3A4 labeling by progesterone analogue Pg-M was obtained from the HPLC-MS-QToF spectra (See Section S5). Percent labeling was calculated by dividing the area under each respective peak corresponding to labeled CYP3A4 species by the sum of the areas under all the peaks corresponding to CYP3A4. Each experiment was performed in at least duplicate and standard deviation is shown by the error bars.

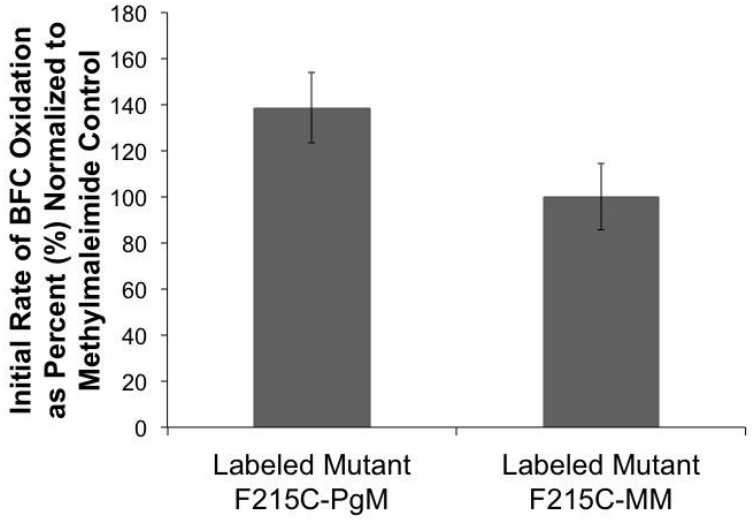

Figure S12. Effect of Pg-M and *N*-methylmaleimide (MM) bioconjugation on Mutant F215C of CYP3A4. Enzyme activity was assayed by measuring the initial rate of enzymatic transformation of BFC. Each sample was treated under bioconjugation condition either in the presence of Pg-M or *N*-methylmaleimide as described in section 2.6 below. The reaction consisted of 0.4 µM CYP3A4, 0.8 µM CPR, 33 µM BFC and 1 mM NADPH in a 100 µL volume. The activity is shown as an average from 3 replicates, normalized to the activity of mutant F215C-MM and the error bars show standard error.

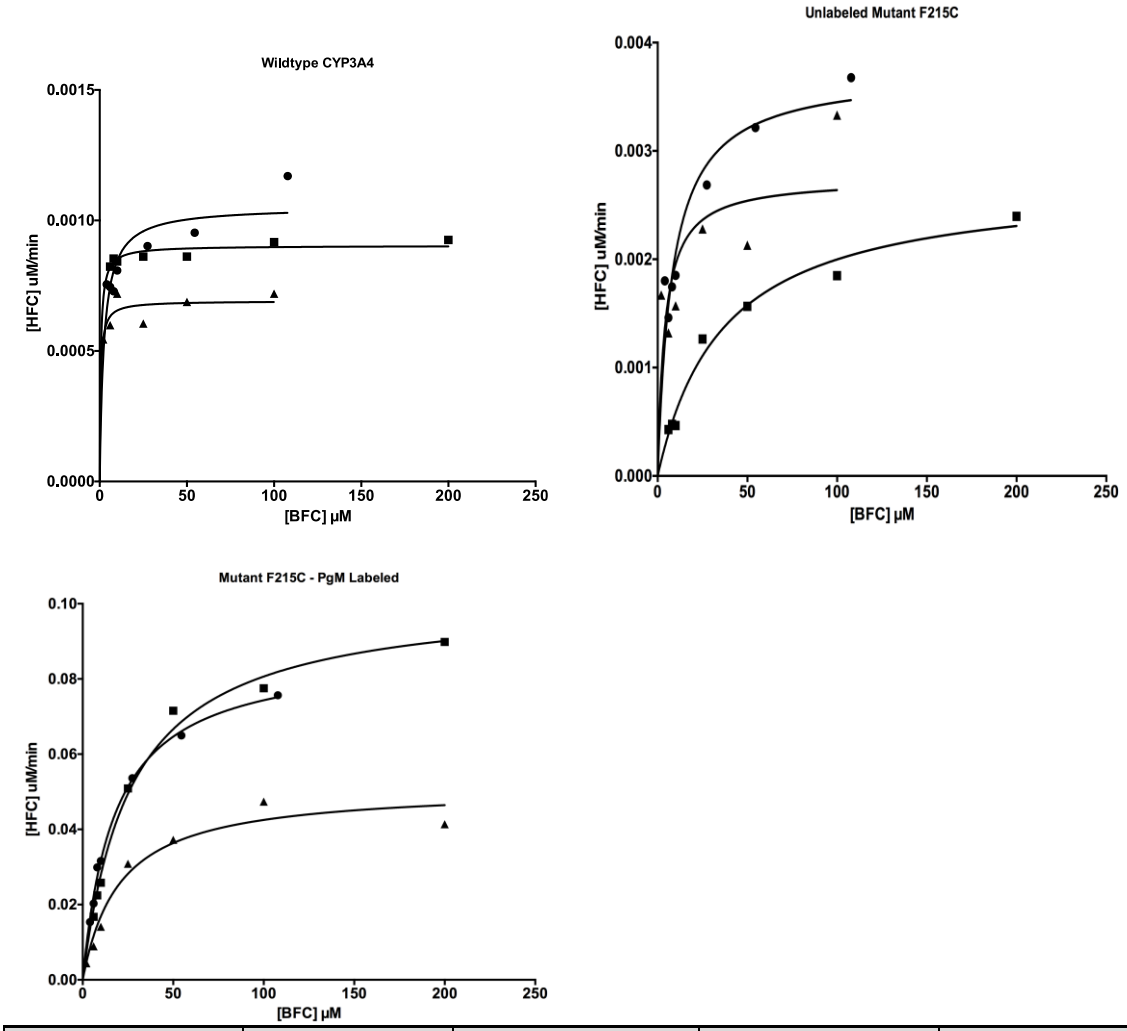

Variant	K_M (µM)	V_{max} (nM/min)	k_{cat} (min^{-1})	R^2
Wildtype	1.2 ± 0.5	0.89 ± 0.04	0.0011 ± 0.0001	0.33
Unlabeled Mutant F215C	9 ± 4	2.9 ± 0.4	0.0036 ± 0.0005	0.38
Labeled Mutant F215C	27 ± 7	90 ± 9	0.11 ± 0.01	0.84

Figure S13. Effect of Pg-M conjugation on Mutant F215C and wildtype CYP3A4 activity at varied BFC concentrations.

Shown are the initial rates of HFC production at varied BFC concentrations. Each enzyme variant is shown in a separate chart and was exposed to bioconjugation conditions either in the presence or absence of Pg-M. Graphs show data points for 3 experiments per sample (different symbols). Data were fitted using a standard hyperbolic (Michaelis-Menten) function using GraphPad Prism Version 6.0e to determine the K_M, V_{max} and k_{cat}, with automatic outlier elimination. Table shows averaged kinetic parameters with standard error, R^2 represents goodness of fit and the $[E]_{total}$ = 0.8 µM.

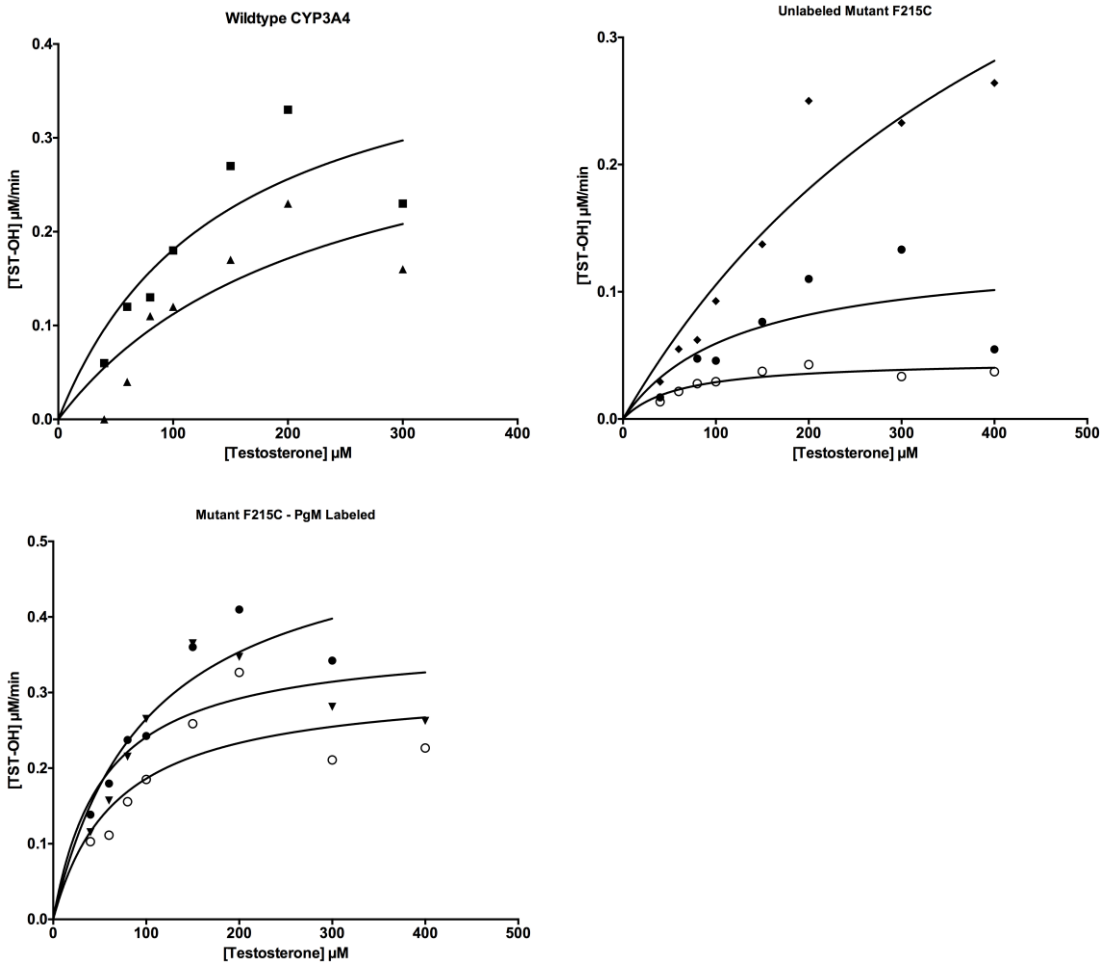

Variant	K_M (µM)	V_{max} (nM/min)	k_{cat} (min^{-1})	R^2
Wildtype	173 ± 126	399 ± 151	0.5 ± 0.2	0.60
Unlabeled Mutant F215C	67 ± 63	90 ± 29	0.11 ± 0.04	0.21
Labeled Mutant F215C	63 ± 25	375 ± 47	0.45 ± 0.06	0.54

Figure S14. Effect of Pg-M conjugation on Mutant F215C and wildtype CYP3A4 activity at varied testosterone concentrations.
Shown are the initial rates of hydroxy-testosterone production at varied testosterone concentrations. Each enzyme variant is shown in a separate chart and was exposed to bioconjugation conditions either in the presence or absence of Pg-M. Data points for 3 experiments per sample are shown, except for wildtype where only two experiments were performed. Data were fitted using a standard hyperbolic (Michaelis-Menten) function using GraphPad Prism Version 6.0e to determine the K_M, V_{max} and k_{cat}, with automatic outlier elimination. Table shows averaged kinetic parameters with standard error, R^2 represents goodness of fit and the $[E]_{total}$ = 0.8 µM. Due to issues with substrate

precipitation in buffer,[2] low enzyme activity and protein aggregation,[3, 4] we were unable to obtain reliable K_M for testosterone (Figure S14).

2. EXPERIMENTAL PROCEDURES: BIOCHEMISTRY

2.1. General Information

All reagents were purchased from Sigma-Aldrich Canada Ltd. (Oakville, ON, Canada), Alfa Aesar (Ward Hill, MA, USA), Chem-Impex (Wood Dale, IL, USA), Agilent Technologies Canada Inc. (Mississauga, ON, Canada) or BioRad (Mississauga, ON, Canada). Reagents were used without further purification. Mutagenesis and sequencing primers were obtained from Life Technologies. CYP3A4 and CPR plasmids were generously provided by Dr. J. R. Halpert (University of Connecticut) and Dr. F. P. Guengerich (Vanderbilt University), respectively. The pEVOL-OpgY plasmid containing the unnatural tRNA and amino acyl tRNA synthetase (aaRS) was kindly donated by Dr. P. G. Schultz (Scripps Research Institute).[5]

2.2. Site Directed Mutagenesis

CYP3A4 mutants were generated using the QuikChange II XL Site-Directed Mutagenesis Kit (Stratagene, Agilent) and the pSE3A4His plasmid encoding N-terminally truncated and tetrahistidine-tagged CYP3A4 wild-type cDNA as the template.[6] Mutations were confirmed using DNA sequencing by Genome Quebec at McGill University (Montreal, Canada). The mutagenesis primers that were used for insertion of the amber stop codon for OPgY mutants are shown in Table S1 to generate mutants: F213OPgY, F215OPgY and F219OPgY. Cysteine depleted mutants were prepared from a previous triple mutant generated in our lab, C98S/C239S/C468G. The PCR primers used for mutagenesis are shown in Table S1.

Table S1: Sequences of mutagenesis primers (forward)

Mutation	Primer
C58T	5'-CCATAAGGGCTTT**AC**TATGTTTGACATGG-3' [7]
C64A	5'-GTTTGACATGGAA**GC**TCATAAAAAGTATGG-3' [7]
L211C	5'-TGGAAAACACCAAGAAGCTTT**GT**AGATTTG-3'
F213C	5'-CCAAGAAGCTTTTAAGAT**G**TGATTTTTTGGATCC-3'
D214C	5'-GGAAAACACCAAGAAGCTTTTAAGATTT**TG**TTTTTTGGATCCATTCTTTCTCTCAA-3'
F215C	5'-GAAAACACCAAGAAGCTTTTAAGATTTGATT**G**TTTGGATCCATTCTTTC-3'
D217C	5'-CCAAGAAGCTTTTAAGATTTGATTTTTTG**TG**TCCATTCTTTCTCTCAATAACAGTCTTT-3'
V240C	5'-CTTGAAGTATTAAATATCAGT**TGC**TTTCCAAGAGAAGTTAC-3'

F213tag	5’- CCAAGAAGCTTTTAAGA**TAG**GATTTTTTGGATCC-3’
F215tag	5’- GCTTTTAAGATTTGAT**TAG**TTGGATCCATTCTTTC-3’
F219tag	5’-TTGGATCCA**TAG**TTTCTCTCAATAACAGTCTTTCC-3’.

2.3. Generation of Cysteine Depleted Mutants

Cysteine depleted mutants were prepared from a previous triple mutant generated in our lab, C98S/C239S/C468G.[8] The PCR primers used for mutagenesis are shown in Table S1. Mutant 1 (C58T/C64A/C98S/C239S/C468G) was first constructed as a starting point to generate the mutants of interest. The following mutants were made by adding a single mutation to mutant 1: L211C, F213C, D214C, F215C, D217C, V214C.

2.4. Expression and purification of wildtype, cysteine depleted mutant, and O-propargyl tyrosine mutant CYP3A4

Wildtype CYP3A4 and cysteine mutants were expressed and purified as previously described, with minor modifications.[8] For protein expression, the cells were harvested at 5000 × g instead of 4000 × g. For lysis, 1.3 µg/mL aprotinin and 1.25% CHAPS were supplemented instead of 1 µg/mL aprotinin and 1% CHAPS, concentrations for the other protease inhibitors were kept the same as published. The lysed sample was split into 3 beakers and sonication was performed at 80% cycle duty instead of 60% cycle duty. Both the Ni-NTA agarose column and Macro-Prep High S Support column were run at a flow rate of 0.6 mL/min instead of 1 mL/min. The protein concentration was calculated from the reduced CO spectrum only, using a molar extinction coefficient of 91 mM^{-1} cm^{-1} between 450 and 490 nm.[8, 9] The O-propargyl tyrosine mutants were expressed with a few modifications. Escherichia coli DH5α competent cells were transformed with both the desired CYP3A4 plasmid and pEVOL-OpgY. Cells were cultured with both 100 µg/mL ampicillin and 25 µg/mL chloramphenicol selection. The growth medium was supplemented with 0.2% w/v L-arabinose and 1 mM O-propargyl tyrosine at the time of induction. Control cultures were grown without the addition of the unnatural amino acid. The protein expression was scaled down to 1/5 of the original volume.

2.5. Expression and purification of Cytochrome P450 Reductase (CPR)

CPR was expressed and purified as previously described with minor changes.[10] For CPR expression, the starting culture was generated by inoculating 100 mL of lysogeny broth (LB) with 8 colonies instead of 6 mL of LB with 4 colonies. The overnight culture was then used to inoculate the bulk culture (12 mL in 1 L instead of 3 mL in 1 L) for 10 L total volume (10 flasks × 1 L). Following expression, the cells were harvested by centrifugation at 3000 × g and resuspended in 0.1 M PBS buffer (10 mL, pH 7.4) before storage at -80ºC. For protein purification, the original protocol was shortened by condensing the two lysis steps into one step and the two sonication steps into one step. In this case, the PBS buffer was removed by centrifugation at 3000 × g and the pellet was resuspended in 40 mL TSE buffer after which lysozyme (1.2 mg in 20 mL TSE buffer) was added and the suspension was incubated for 20 min at 4ºC. The lysate was centrifuged at 3000 × g for 30 min and 4ºC, and the pellet was resuspended in lysis

buffer (60 mL). Sonication was performed in 7 cycles at 60% cycle duty, power 8 for 30 sec and the homogenate was centrifuged at 73 000 × g for 45 min at 4°C. The supernatant was supplemented with 1 mM PMSF and loaded on a 2′,5′ADP Sepharose 4B column (GE Healthcare Life Sciences). The concentration of holo-CPR was determined by measuring its flavin content using the $K_3Fe(CN)_6$ assay with an extinction coefficient of 21.4 mM^{-1} cm^{-1} at 455 nm, and activity by measuring the reduction of cytochrome c. [10]

2.6 Measurement of BFC transformation

Initial rates for CYP3A4-catalyzed transformation of 7-benzyloxy-4-trifluoromethyl coumarin (BFC) were measured by monitoring the production of 7-hydroxy-4-trifluoromethyl coumarin (HFC) using a microtitre plate fluorimeter (SpectraMax i3, Molecular Devices). The assay was performed by combining CYP3A4 (0.4 µM), CPR (either 0.8 µM or 1.6 µM) and BFC (33 µM, from a 10 mM stock in ACN) in 0.1 M potassium phosphate buffer at pH 7.4, such that there was < 1 % solvent in the reaction. The mixture was incubated at 37°C for 5 min, before reaction initiation with NADPH (1 mM or 10 mM, from a 25 mM stock in H_2O). HFC production was monitored for 1 h with measurements taken every 30 sec with HFC excitation at 410 nm and detection of emission at 530 nm. The initial rate was determined from the slope of the linear segment at the beginning of the kinetic curve, and RFU converted to [HFC] using a calibration curve.

Experiments where BFC concentration was varied were monitored using a microtitre plate fluorimeter (Synergy 2, BioTek Instruments) The assay was performed by combining CYP3A4 (0.8 µM), CPR (1.6 µM) and BFC (2 - 100 µM, from either 0.5 or 5 mM stocks in DMSO) in 0.1 M potassium phosphate buffer at pH 7.4, such that there was < 2 % solvent in the reaction. The mixture was incubated at 37°C for 5 min, before reaction initiation with NADPH (950 µM, from a stock in H_2O). HFC production was monitored for 3 h with measurements taken every 30 sec with HFC excitation at 410 nm and detection of emission at 530 nm. The initial rate was determined from the slope of the linear segment at the beginning of the kinetic curve, and RFU converted to [HFC] using a calibration curve.

2.7 Measurement of testosterone hydroxylation.

The CYP3A4 turnover was also assayed by measuring the end-point production of hydroxytestosterone from testosterone using HPLC-MS (Agilent Technologies) using an established protocol.[10] For the fluorophore-enzyme conjugates, the assay was performed by combining the enzyme conjugate (0.4 µM), testosterone (115 µM, 0.69 µL from a 25 mM stock in MeOH) and cumene hydroperoxide (CHP, 2 × 600 µM)[10] in potassium phosphate buffer (0.1 M, pH 7.4) for 1 h at 37°C and gentle shaking at 250 RPM. The enzyme and testosterone were pre-incubated in buffer at 37°C for 10 min before the reaction was initiated with the addition of CHP. CHP was supplemented again after 15 min. For the progesterone conjugates the assay was performed by combining the modified enzyme (0.4 µM), testosterone (180 µM, 1.8 µL from 10 mM stock in DMSO) and CPR (0.8 µM) in potassium phosphate buffer (0.1 M, pH 7.4) for 5 min at 37°C,

before initiation of the reaction with NADPH (1.1 mM). The reaction was allowed to proceed for 1 h at 37°C with orbital shaking at 250 RPM before quenching. In both cases, the reaction was quenched with dichloromethane (DCM, 500 µL) and the internal standard cortexolone (20 µM), after which the product was extracted in DCM (3 × 500 µL). The combined extracts were evaporated and the residue was redissolved in acetonitrile (ACN, 100 µL) in preparation for HPLC-MS analysis. The separation and quantification of the products was achieved using an Eclipse XDB-C18 (5 µm, 4.6 × 150 mm) column in line with a UV detector (set to monitor at 244 nm) and mobile phases A (Milli-Q water) and B (ACN) at a flow rate of 0.5 mL/min. The elution entailed an isocratic step at 50% phase B for 5 min, followed by an increase to 70% phase B over 7 min before an increase to 95% phase B over 8 min. The retention times were: 3.6 min for the major product 6β-hydroxytestosterone, 3.3 min, 3.9 min and 4.6 min for the minor hydroxylated testosterone products (likely 1β-hydroxytestosterone, 2β-hydroxytestosterone, 15β-hydroxytestosterone as suggested by Guengerich et al.[11]), 5.0 min for cortexolone and 7.7 min for testosterone. Product yield was calculated as a percentage by dividing the sum of the areas under the peaks of the products by the sum of the areas under the peaks of the products and testosterone starting material combined.

Experiments where CYP3A4 activity toward testosterone was measured and the testosterone concentration was varied, the amounts of hydroxy-testosterone produced at set time points were quantified using HPLC-MS. The assay was performed by combining the modified enzyme (0.8 µM), testosterone (40-400 µM, from 10 mM and 100 mM stocks in DMSO) and CPR (0.8 µM) in potassium phosphate buffer (0.1 M, pH 7.4) for 5 min at 37°C, before initiation of the reaction with NADPH (1.0 mM). Care was taken such that there was < 2 % solvent in the reaction. The reaction was incubated at 37°C with orbital shaking at 350 RPM before quenching. Aliquots (100 µL) were taken at 5 min intervals for 30 min, and quenched in ACN (100 µL) spiked with cortexolone (10 µM, internal standard) by vortexing for 30 sec. The quenched samples were pelleted for 30 min at 14 000 × g and filtered in preparation for HPLC-MS analysis. The separation and quantification of the products was achieved using an Eclipse XDB-C18 (5 µm, 4.6 × 150 mm) column in line with a UV detector (set to monitor at 244 nm) and mobile phases A (Milli-Q water) and B (ACN) at a flow rate of 0.5 mL/min. The elution entailed an isocratic step at 100% phase A for 3 min, followed by an increase to 95% phase B over 12 min before an isocratic step at 95% phase B over 5 min. The retention times were: 13.7 min for the major product 6β-hydroxytestosterone, 13.3 min, 14.2 min and 14.9 min for the minor hydroxylated testosterone products (likely 1β-hydroxytestosterone, 2β-hydroxytestosterone, 15β-hydroxytestosterone as suggested by Guengerich et al.[11]), 15.2 min for cortexolone and 16.5 min for testosterone. Product yield was calculated by converting the sum of the areas under the peaks of the products to amount of hydroxylated product (µM) using a calibration curve. The rate of hydroxylation was determined from the linear portion at the beginning of the kinetic curve.

2.8 Labeling of *O*-propargyl tyrosine mutant CYP3A4 with azide containing fluorophores

Premixed $CuSO_4$: tris(3-hydroxylpropyltriazolylmethyl)amine (100:500 µM from a 13.3:66.7 mM stock in H_2O) was added to KPi buffer (0.1 M, pH 7.4) containing azide-fluorophore (200 µM from a 20 mM stocking in DMSO) and the desired CYP3A4 variant (2 µM). The reaction was next supplemented with aminoguanidine (5 mM from a 200 mM stock in H_2O), initiated with sodium ascorbate (5 mM from a 200 mM stock in H_2O) and reacted for 1 h at 30°C and 250 RPM orbital shaking. The reaction was quenched by removal of the reagents with Zeba Desalting Columns (3 × 0.5 mL, Pierce). Conjugation was confirmed via stain-free SDS-PAGE and fluorescent imaging of conjugated fluorophores. An aliquot (20 µL) of the conjugation reaction was run on a 12% Mini-Protean gel (Bio-Rad). The proteins were visualized using the ChemiDoc MP fluorescent imager (Bio-Rad); total protein using the Stain Free setting, and each fluorophore with its respective settings.

2.9 Labeling of cysteine-depleted mutant CYP3A4 with maleimide-containing small molecules

CYP3A4 wildtype and mutants were covalently labeled with small molecules (fluorophores or progesterone analogue) containing a maleimide moiety using the following general protocol modified from Menard et al.[8] The desired CYP3A4 variant (1 µM) was incubated with TCEP (45 µM from a 10 mM stock in H_2O) at room temperature for 20 min on an orbital shaker (50 RPM), in a glass vial. The reaction was initiated with the addition of the desired maleimide derivative (100 µM from a 20 mM stock solution in anhydrous DMSO) and allowed to proceed at 4°C, for 2 h with gentle shaking. The reaction was quenched with DTT (2 mM from a 100 mM stock in H_2O) for 10 min at r.t., then desalted with Zeba Spin Desalting Columns (3 × 0.5 mL, Pierce). For progesterone labeled samples, a reaction volume of 700 µL was used and the sample was desalted with Zeba Spin Desalting Columns (1 × 2 mL, Pierce). Control reactions were treated in the same manner without the addition of small molecules but pure DMSO instead. Conjugation was confirmed via stain-free SDS-PAGE and fluorescent imaging of conjugated fluorophores. An aliquot (10 µL) of the conjugation reaction was run on a 12% Mini-Protean gel (Bio-Rad). The proteins were visualized using the ChemiDoc MP fluorescent imager (Bio-Rad); total protein using the Stain Free setting, and each fluorophore with its respective settings.

2.10 Determination of labeling yields using HPLC-MS-QToF

Labeling yields were calculated using an LC system coupled to a MS-QToF. Following labeling, the sample was washed with H_2O (3 × 0.5 mL) using a Spin-X UF concentrator (30K MWCO, Corning) for 15 min at 15000 × g. The intact proteins were analyzed by LC-MS using a Dionex Ultimate 3000 HPLC system coupled to a Bruker Maxis Impact QToF MS in positive ESI mode. Samples were run through a Poros R2/10 column from Applied Biosystems (10 µm, 2000 Å, 2.1 × 100 mm) using a gradient of 90% mobile phase A (0.1% formic acid in water) and 10% mobile phase B (0.1% formic acid in acetonitrile) to 0% mobile phase A and 100% mobile phase B in 15 min. The data was processed and deconvoluted using the Bruker DataAnalysis software version 4.1.

2.11 Determination of regioselectivity using cyanogen bromide digestion and tricine-SDS-PAGE

To confirm the regioselectivity of the labeling, samples conjugated to fluorophores were subjected to an in-gel cyanogen bromide (CNBr) digestion[8, 12] and the peptides were analyzed using tricine-SDS-PAGE[13] and fluorimetry. Labeled protein samples were loaded onto a 12% tricine SDS-PAGE gel, followed by staining (0.2% Coomassie Brilliant Blue-G250, 20% MeOH, 0.5% acetic acid) and destaining (30% aqueous MeOH). The band at about 56 kDa was next excised, washed (2 × 150 µL 50% aqueous ACN, 20 min, 37ºC, 250 rpm) and dried using a SpeediVac. CNBr (150 µL, 16 mg/mL in 70% formic acid) was added to the gel pieces in polypropylene tubes and left to incubate at r.t. for 48 h in the dark. The reaction was quenched by evaporation of the reagent and solvent using the SpeediVac. The residue was washed (2 × 150 µL Milli-Q H_2O), with sonication (5 min) applied between washings and dried using a SpeediVac. The residue thus obtained (containing the peptides) was dissolved in 1 × Laemmli Sample Buffer (50 µL, Bio-Rad), heated (75-100ºC, 3 min) and loaded on a 10-20% Mini-PROTEAN Tris-Tricine gel (Bio-Rad). The gel was run in 1 × Tris/Glycine/SDS buffer (BioRad) at 30 V for 30 min, followed by 90 V for ~ 3 hours, or until the dye front reached the end of the gel. Peptides were visualized before staining (as described in section 1.5) and after staining with SyproOrange to account for fluorescence quenching.

2.12 Effect of quenched maleimide ligands on enzymatic activity

To check whether the small molecules were attaching to the enzyme in a mechanism different than the thiolate-maleimide reaction, maleimide-containing molecules were quenched with DTT (2 mM) for 45 min. CYP3A4 was added to the mixture together with TCEP and the samples were treated as in section 2.9.

3. EXPERIMENTAL PROCEDURES: SYNTHESIS

3.1. General Information

All reagents were purchased from Sigma-Aldrich Canada Ltd. (Oakville, ON, Canada), Alfa Aesar (Ward Hill, MA, USA), Chem-Impex (Wood Dale, IL, USA) or Toronto Research Chemicals (Toronto, ON, Canada). Reagents were used without further purification. Dry solvents were obtained from an Innovative Tech Pure Solve MD-7 solvent purification system. Reactions were performed in flame-dried glassware under an argon or N_2 atmosphere. Thin Layer Chromatography (TLC) analysis was performed using 60 Å F_{254} silica-coated plates from Silicycle (Quebec City, QC, Canada). Flash chromatography was performed using a CombiFlash Rf system (Gold columns) from Teledyne Isco (Lincoln, NE, USA). ^{1}H and ^{13}C NMR spectra were recorded on Varian 300, 400 MHz or Bruker 500 MHz spectrometers with the data reported in conventional form: chemical shifts (δ ppm), coupling constants (Hz), multiplicity (s – singlet, d – doublet, t – triplet, q – quartet, p – pentet, m – multiplet, br – broad). For signal determination additional spectra such as 2D (^{1}H-^{1}H-COSY, ^{1}H-^{13}C-HSQC, ^{1}H-^{13}C-HMBC) were recorded. High-resolution mass spectra were obtained from the McGill

University Mass Spectral Facility by ESI on a Thermo Fisher Scientific Inc. Exactive orbitrap system. Synthesis of *O*-propargyl tyrosine (**3**) was modified from Deiters *et al.*[14]

3.2. Synthesis of *O*-propargyl tyrosine (3)

Scheme S1. Synthesis of *O*-propargyl tyrosine (3) [14]

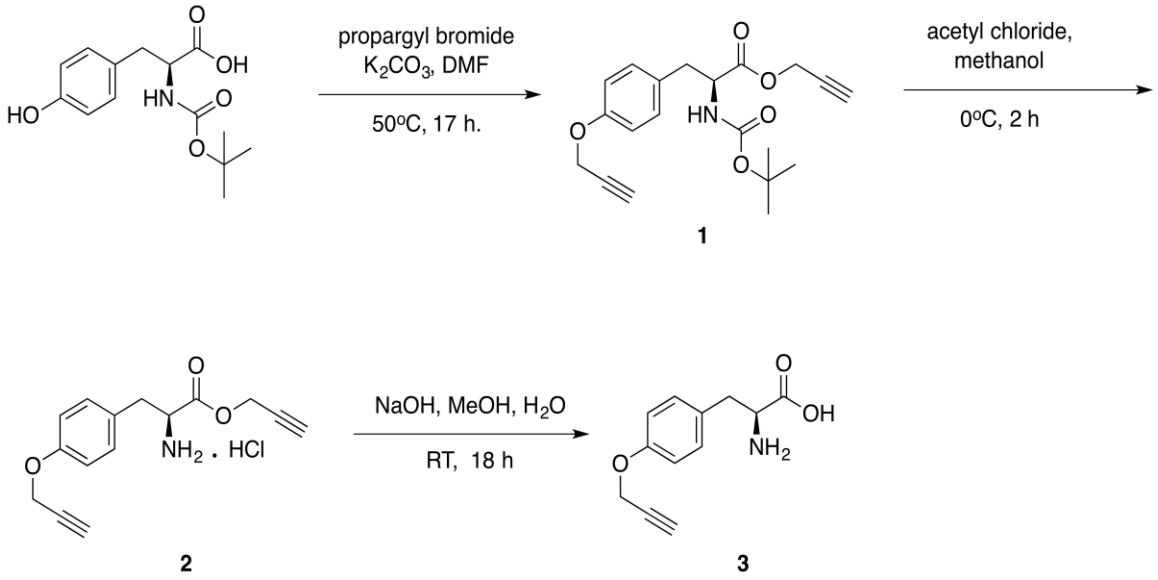

3.2.1. 2-*tert*-Butoxycarbonylamino-3-[4-(prop-2-ynyloxy)phenyl]-propionic acid propargyl ester (1)

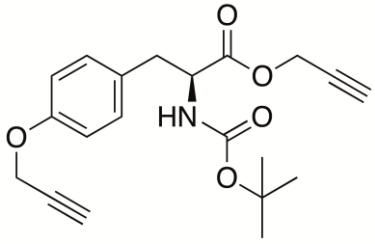

N-*tert*-Butoxycarbonyl-tyrosine (10.0 g, 36.6 mmol, 1.0 eq.) and K_2CO_3 (19.7 g, 142.0 mmol, 4.0 eq.) were suspended in dry DMF (71 mL) under N_2 and stirred for 10 min at 50ºC. Propargyl bromide (10.5 mL, 118.0 mmol, 3.3 eq.) was slowly added and the reaction was allowed to stir for 17 h. Following reaction completion, the K_2CO_3 was filtered off, water (200 mL) was added to the reaction and the product was extracted in ethyl acetate (3 × 200 mL). The combined organic layers were concentrated (~100 mL), washed with water (3 × 100 mL), brine (100 mL) and dried over anhydrous Na_2SO_4 before filtration and solvent evaporation *in vacuo.* The product was obtained as a yellow oil (13.6 g) that was used in the next step without further purification. ^{1}H NMR (400 MHz, Chloroform-*d*) δ = 7.09 (d, *J* = 8.6 Hz, 2H), 6.90 (d, *J* = 8.6 Hz, 2H), 4.93 (d, *J* = 7.9 Hz, 1H), 4.63 – 4.82 (m, 4H), 4.59 (q, *J* = 6.1 Hz, 1H), 2.99-3.14 (m, 2H), 2.51 (t overlapped, *J* = 2.5 Hz, 1H), 2.51 (t overlapped, *J* = 2.4 Hz, 1H), 1.42 (s, 9H).

3.2.2. 2-Amino-3-[4-(prop-2-ynyloxy)phenyl]-propionic acid propargyl ester (2)

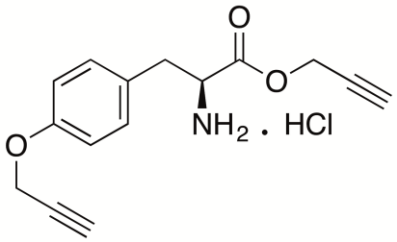

Acetyl chloride (45.5 mL, 640 mmol, 17.6 eq.) was slowly added to dry methanol (100 mL) at 0°C on an ice-salt-water bath under N_2 atmosphere to generate anhydrous HCl *in situ*. Compound **1** (13.0 g, 36.4 mmol, 1.0 eq.) was pre-dissolved in methanol (15 mL) before addition to the methanolic HCl solution. The reaction was stirred at 0°C for 2 h. It was next allowed to warm to room temperature before evaporation of the solvent *in vacuo*. The greenish-white product (24.9 g) was used in the next step without further purification. The ^{1}H NMR spectrum matched the literature.[15] ^{1}H NMR (300 MHz, DMSO-d_6) δ = 7.33 (brs, 3H), 7.17 (d, *J* = 8.7 Hz, 2H), 6.93 (d, *J* = 8.7 Hz, 2H), 4.71 – 4.85 (m, 4H), 4.30 (t, *J* = 6.4 Hz, 1H), 3.69 (t, *J* = 2.4 Hz, 1H), 3.58 (t, *J* = 2.3 Hz, 1H), 3.05 (m, 2H).

3.2.3. *O*-Propargyl tyrosine (3)

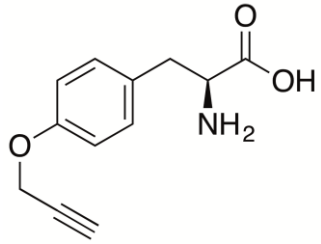

Compound 2 (24.9 g) was dissolved in a solution of methanol (67 mL) and 2 M NaOH (95 mL). The reaction was stirred for 18 h at room temperature before neutralization with conc. HCl. The beige precipitate was left to grow at 4°C overnight before filtration and drying *in vacuo* to yield a beige powder (5.3 g, 66% over 3 steps). ^{1}H NMR spectrum matched the literature.[14, 15] ^{1}H NMR (300 MHz, DMSO-d_6) δ = 7.49 (brs, 2H), 7.19 (d, *J* = 8.6 Hz, 2H), 6.89 (d, *J* = 8.6 Hz, 2H), 4.75 (d, *J* = 2.4 Hz, 2H), 3.56 (t, *J* = 2.3 Hz, 1H), 3.33 (dd, *J* = 8.2 Hz, *J* = 4.4 Hz, 1H), 3.07 (dd, *J* = 14.3 Hz, *J* = 4.3 Hz, 1H), 2.79 (dd, *J* = 14.3 Hz, *J* = 8.3 Hz, 1H).

3.3. Synthesis of *N*-(*N*'-ethylmaleimide)-17β-testosterone carboxamide (Pg-M).

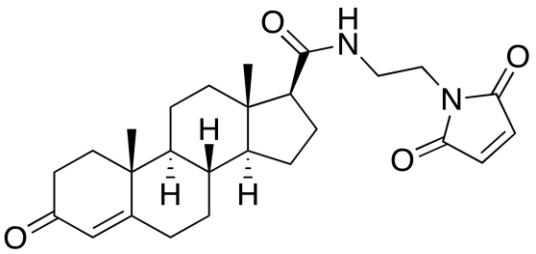

N-(2-aminoethyl)maleimide trifluoroacetate salt (32.4 mg, 0.127 mmol, 2.0 eq.) was added to 17β-testosterone carboxylic acid (19.8 mg, 0.063 mmol, 1.0 eq., purchased from

Toronto Research Chemicals, Cat. No. T155070), HATU (49.4 mg, 0.130 mmol, 2.1 eq.), and diisopropylethylamine (0.022 mL, 0.129 mmol, 2.1 eq.) in dry dimethylformamide (1 mL) under anhydrous conditions. The reaction was performed in a μwave at 60°C for 30 min, normal absorptivity setting. Following completion, the reaction was diluted in sat. NH4Cl (100 mL) and extracted with DCM (3 × 100 mL), the DCM was removed in vacuo and the product was redissolved in EtOAc (50 mL), washed with sat. NH4Cl (3 × 50 mL), dried with anhydrous sodium sulfate before removing the solvent in vacuo. The product was purified using silica gel column chromatography (DCM/MeOH ranging from 100/0 to 97:3) to afford Pg-M as a white powder (5.7 mg, 0.013 mmol, 21%). ^{1}H NMR (500 MHz, $CDCl_3$) δ = 6.72 (s, 2H), 5.77 – 5.64 (s overlapped, 2H), 3.75 – 3.64 (m, 2H), 3.56 – 3.41 (m, 2H), 2.47 – 2.22 (m, 4H), 2.16 – 1.98 (m, 3H), 1.95 (ddd, J =12.3 Hz, J = 4.0 Hz, J = 2.8 Hz, 1H), 1.90 – 1.82 (m, 1H), 1.80 – 1.65 (m, 3H), 1.64 – 1.49 (m, 2H, overlapped with H_2O), 1.44 (dddd, J =13.0 Hz, J = 4.0 Hz, 1H), 1.37 – 1.19 (m, 3H, overlapped with IPA), 1.18 (s, 3H), 1.12 – 0.99 (m, 2H) 0.95 (ddd, J =12.3 Hz, J = 10.7 Hz, J = 4.2 Hz), 0.70 (s, 3H); ^{13}C NMR (126 MHz, $CDCl_3$) δ = 199.59, 173.19, 171.15, 171.05, 134.39, 124.06, 57.11, 55.66, 53.92, 43.81, 39.02, 38.77, 38.29, 37.94, 35.90, 35.77, 34.11, 32.95, 32.09, 24.51, 23.84, 21.06, 17.54, 13.25; HRMS (ESI): $[M+Na]^+$ calculated for $C_{26}H_{34}O_4N_2Na$: 461.23108, found: 461.24038; R_f = 0.2 (toluene/ethyl acetate/acetone = 6/1/1).

4. PG-M SPECTRA

4.1. ^{1}H NMR (500 MHz, Chloroform-*d*): N-(N'-ethylmaleimide)-17α-testosterone carboxamide (Pg-M)

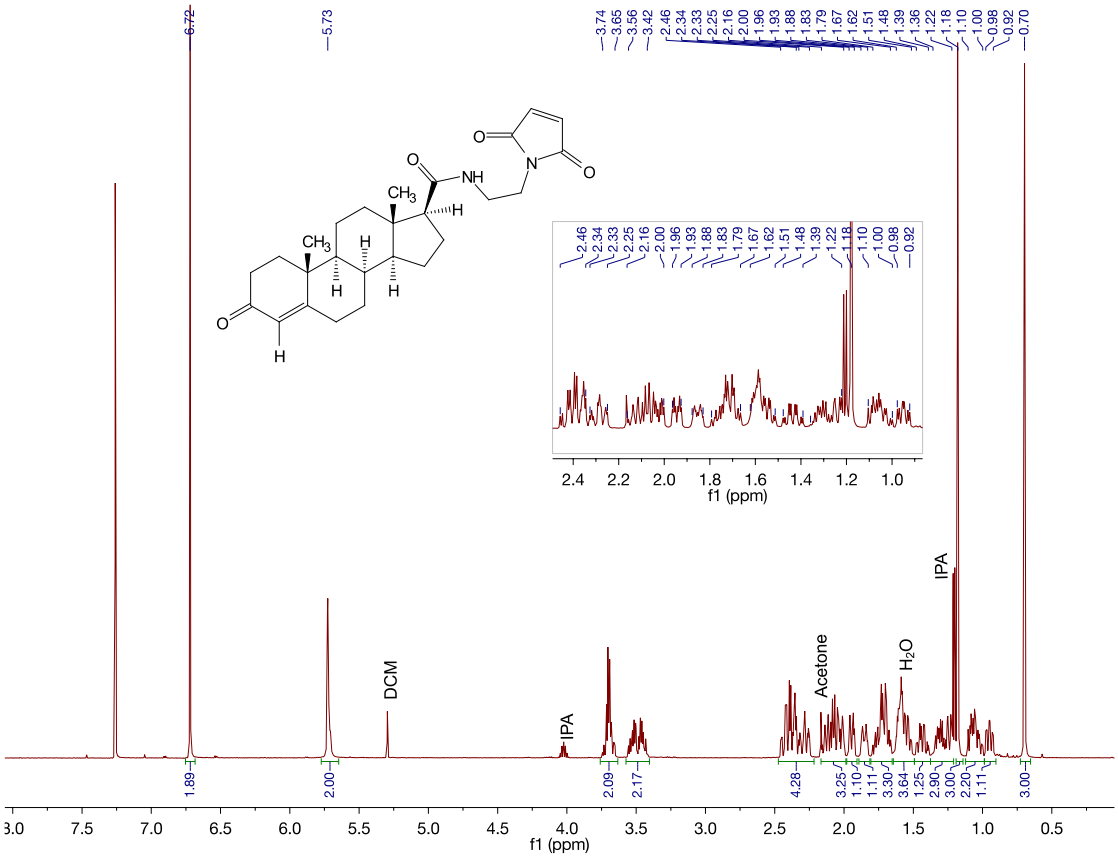

4.2. ^{13}C NMR (126 MHz, Chloroform-*d*): N-(N'-ethylmaleimide)-17α-testosterone carboxamide (Pg-M)

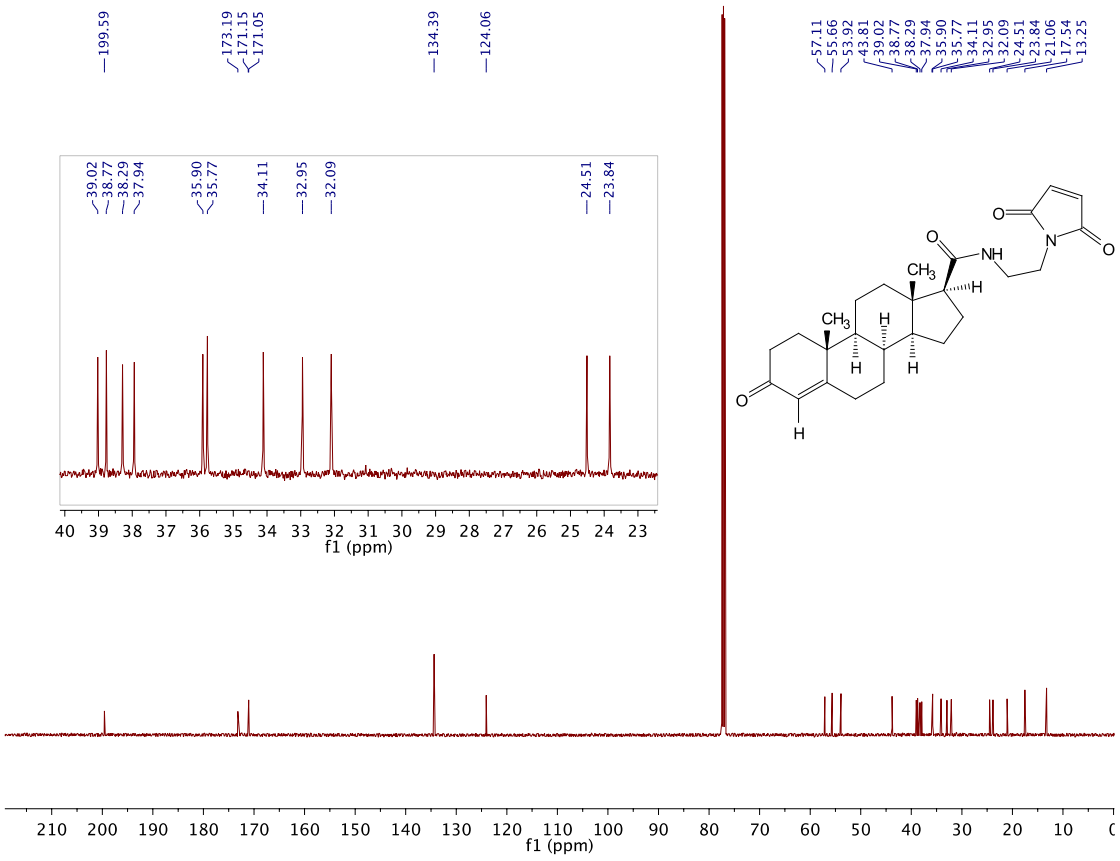

4.3. HPLC Purity Spectra

The purity of Pg-M was confirmed using HPLC with two difference methods, as described below. The separation and quantification of the product was achieved using an Eclipse XDB-C18 (5 µm, 4.6 × 150 mm) column in line with a UV detector (set to monitor at 244 nm) and mobile phases A (Milli-Q water) and B (acetonitrile) at a flow rate of 0.5 mL/min.

Method A: The elution entailed an isocratic step at 50% phase B for 5 min, followed by an increase to 70% phase B over 7 min before an increase to 95% phase B over 8 min. The product eluted at 6.496 min with < 5% impurity at 3.065 min.

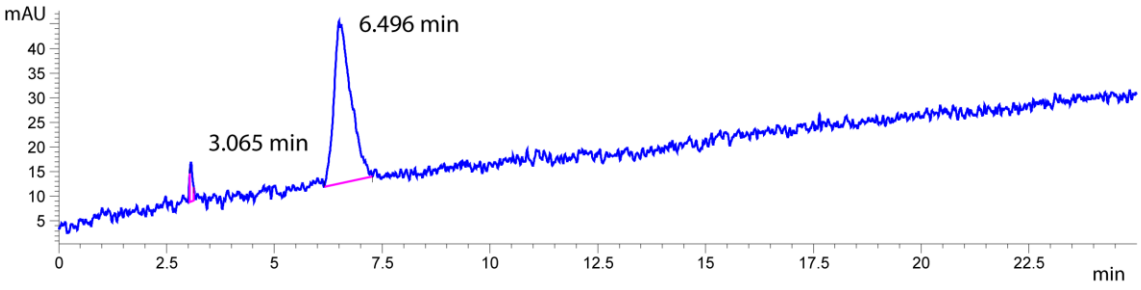

Method B: The elution entailed a gradient step from 5% phase B to 50% phase B over 10 min, followed by an increase to 70% phase B over 5 min before an increase to 95% phase B over 5 min. The product eluted at 17.077 min with no visible impurities.

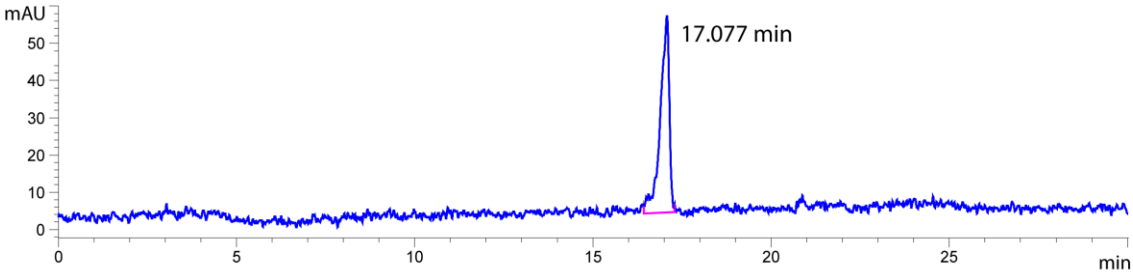

5. DECONVOLUTED MASS SPECTRA FOR CYP3A4 CONJUGATES

Theoretical protein average mass was determined using the Compute pI/Mw Tool from ExPASy: Bioinformatics Resource Portal. The difference in mass between the theoretical mass and detected mass of ~ 27 amu likely corresponds to formylation of the protein upon expression.[16] The standard deviation is determined from at least duplicate samples, unless marked by N.A. Area under curve is comparable under the assumption that different labeling events do not affect the ionization capabilities of the conjugates for large proteins with many charged states.

5.1. Masses of unmodified enzymes

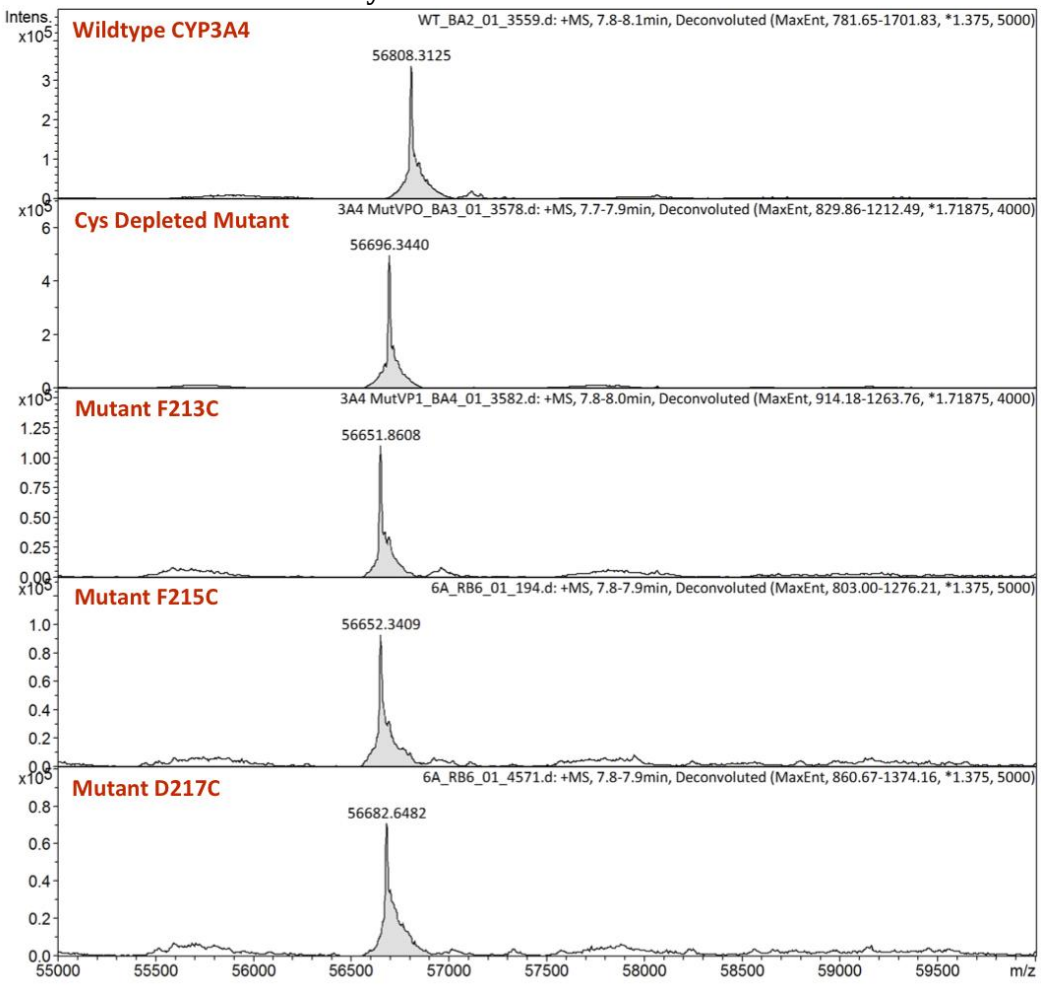

Enzyme	Theoretical Mass	Average Observed Mass	Standard Deviation
Wildtype	56781.45	56808.58555	0.35196
Cys Depleted Mutant	56669.15	56696.35155	0.01068
Mutant F213C	56625.11	56652.57817	0.78760
Mutant F215C	56625.11	56652.42701	0.36081
Mutant D217C	56669.15	56682.81911	0.47001

5.2. Protein conjugates after labeling mutant F213C with fluorophores

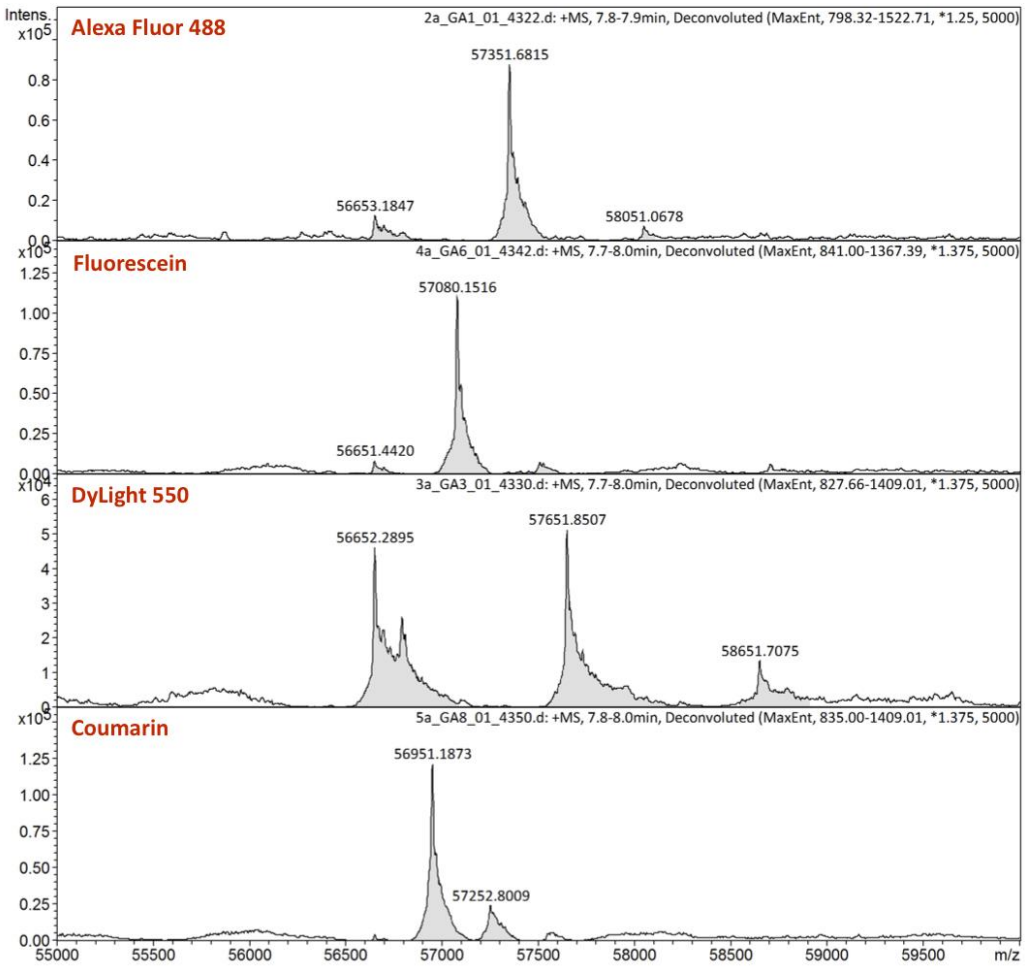

Fluorophore	No. of Fluorophores	Theoretical Mass	Average Observed Mass	Standard Deviation
Unlabeled Protein	0	56625.11	56652.57817	0.78760
Alexa Fluor 488	1	57345.77	57351.29218	0.289175
+ 699 amu	2	58066.43	58050.57308	0.814981
	3	58787.09	58750.44610	3.048160
Fluorescein	1	57052.51	57079.90652	0.174391
+ 427 amu	2	57479.91	57507.85148	0.499518
	3	57907.31	N.A.	N.A.
DyLight 550	1	57690.11	57652.91807	1.67809
+ 1000 amu	2	58755.11	58652.15540	0.417994
	3	59820.11	N.A.	N.A.
Coumarin	1	56923.41	56951.43470	0.24195
+ 298 amu	2	57221.71	57252.14623	1.11983
	3	57520.01	N.A.	N.A.

5.3. Protein conjugates after labeling mutant F215C with fluorophores

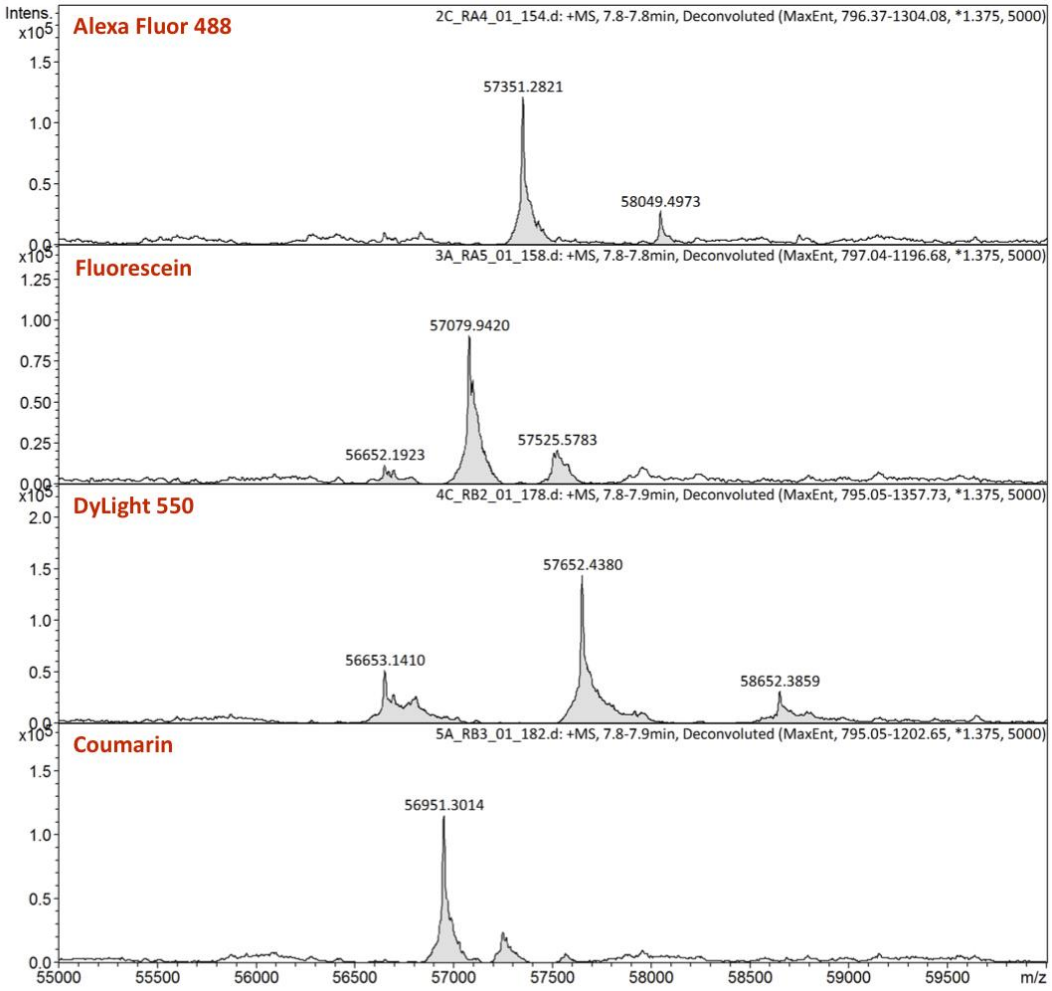

Fluorophore	No. of Fluorophores	Theoretical Mass	Average Observed Mass	Standard Deviation
Unlabeled Protein	0	56625.11	56652.48366	0.34982
Alexa Fluor 488	1	57345.77	57351.05843	0.19535
+ 699 amu	2	58066.43	58049.85170	0.62452
	3	58787.09	56835.36360	N.A.
Fluorescein	1	57052.51	57079.97053	0.24883
+ 427 amu	2	57479.91	57525.72560	0.13906
	3	57907.31	57953.54410	N.A.
DyLight 550	1	57690.11	57652.32800	0.34251
+ 1000 amu	2	58755.11	58652.71997	0.31730
	3	59820.11	N.A	N.A.
Coumarin	1	56923.41	56951.13143	0.62909
+ 298 amu	2	57221.71	57249.89357	0.62909
	3	57520.01	57569.42517	2.22369

5.4. Protein conjugates after labeling mutant D217C with fluorophores

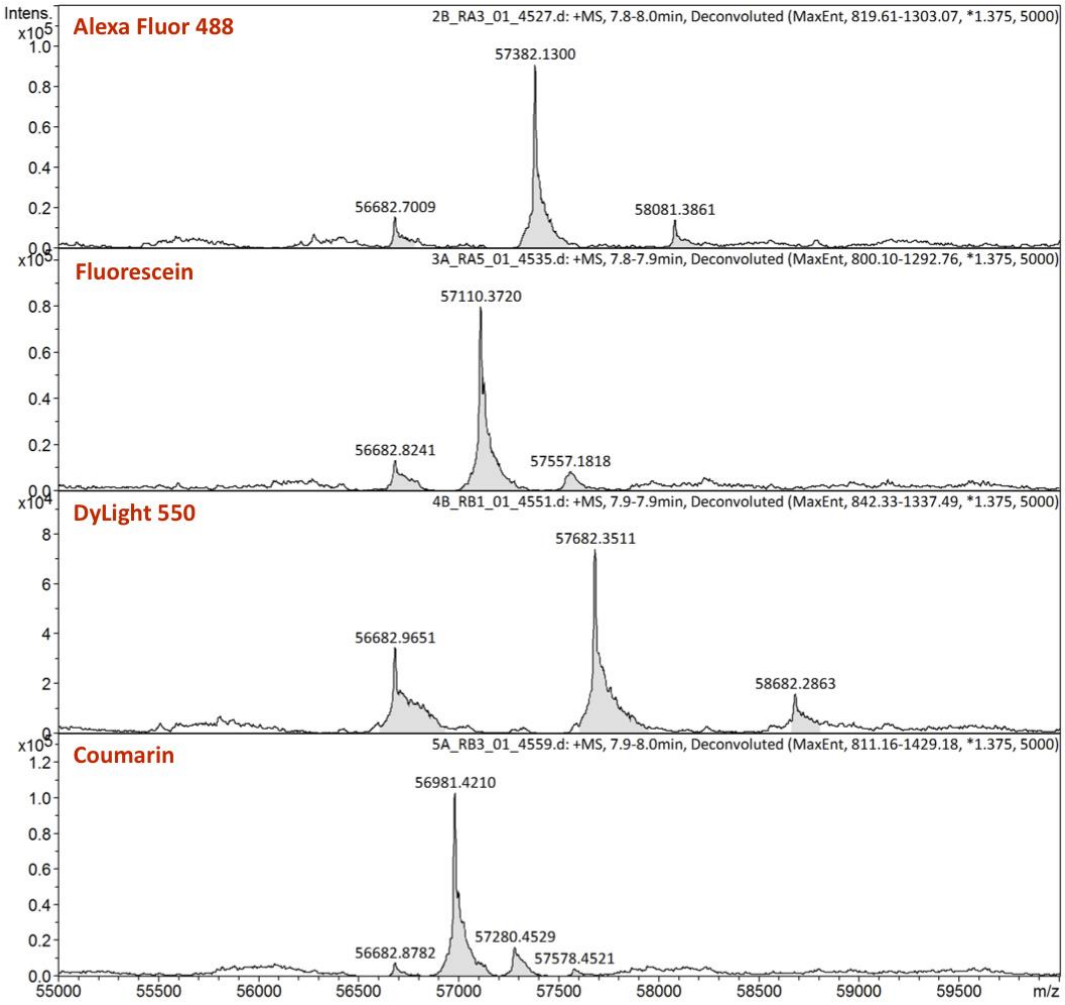

Fluorophore	No. of Fluorophores	Theoretical Mass	Average Observed Mass	Standard Deviation
Unlabeled Protein	0	56669.15	56683.43651	0.70080
Alexa Fluor 488	1	57345.77	57351.05843	0.19535
+ 699 amu	2	58066.43	58049.85170	0.62452
	3	58787.09	56835.36360	N.A.
Fluorescein	1	57052.51	57079.97053	0.24883
+ 427 amu	2	57479.91	57525.72560	0.13906
	3	57907.31	57953.54410	N.A.
DyLight 550	1	57690.11	57652.32800	0.34251
+ 1000 amu	2	58755.11	58652.71997	0.31730
	3	59820.11	N.A.	N.A.
Coumarin	1	56923.41	56951.13143	0.27345
+ 298 amu	2	57221.71	57249.89357	0.62909
	3	57520.01	57569.42517	2.22369

5.5. Protein conjugates after labeling wildtype and different mutants of CYP3A4 with Pg-M

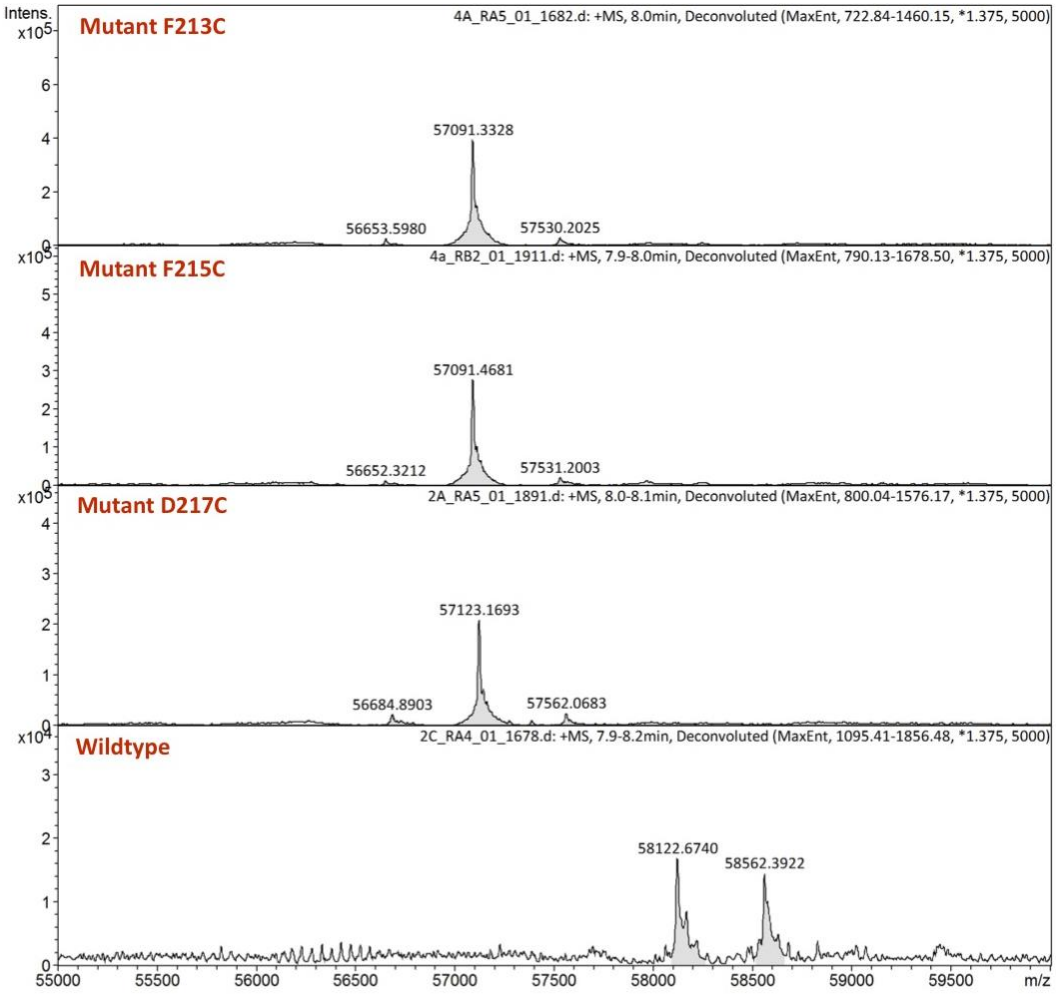

Fluorophore	No. of Fluorophores	Theoretical Mass	Average Observed Mass	Standard Deviation
Wildtype	0	56781.45	56808.58555	0.35196
	3	58097.16	58123.17833	0.47468
	4	58535.73	58564.39457	3.32292
Mutant F213C	0	56625.11	56652.57817	0.78760
	1	57063.68	57091.40110	0.07292
	2	57502.25	57531.50007	1.54338
Mutant F215C	0	56625.11	56652.48366	0.34982
	1	57063.68	57091.38040	0.12403
	2	57502.25	57531.89675	0.98493
Mutant D217C	0	56669.15	56683.43651	0.70080
	1	57107.72	57123.15793	0.04572
	2	57546.29	57562.31790	0.24373

5.6. Mass of mutant CYP3A4 after reaction with quenched Pg-M

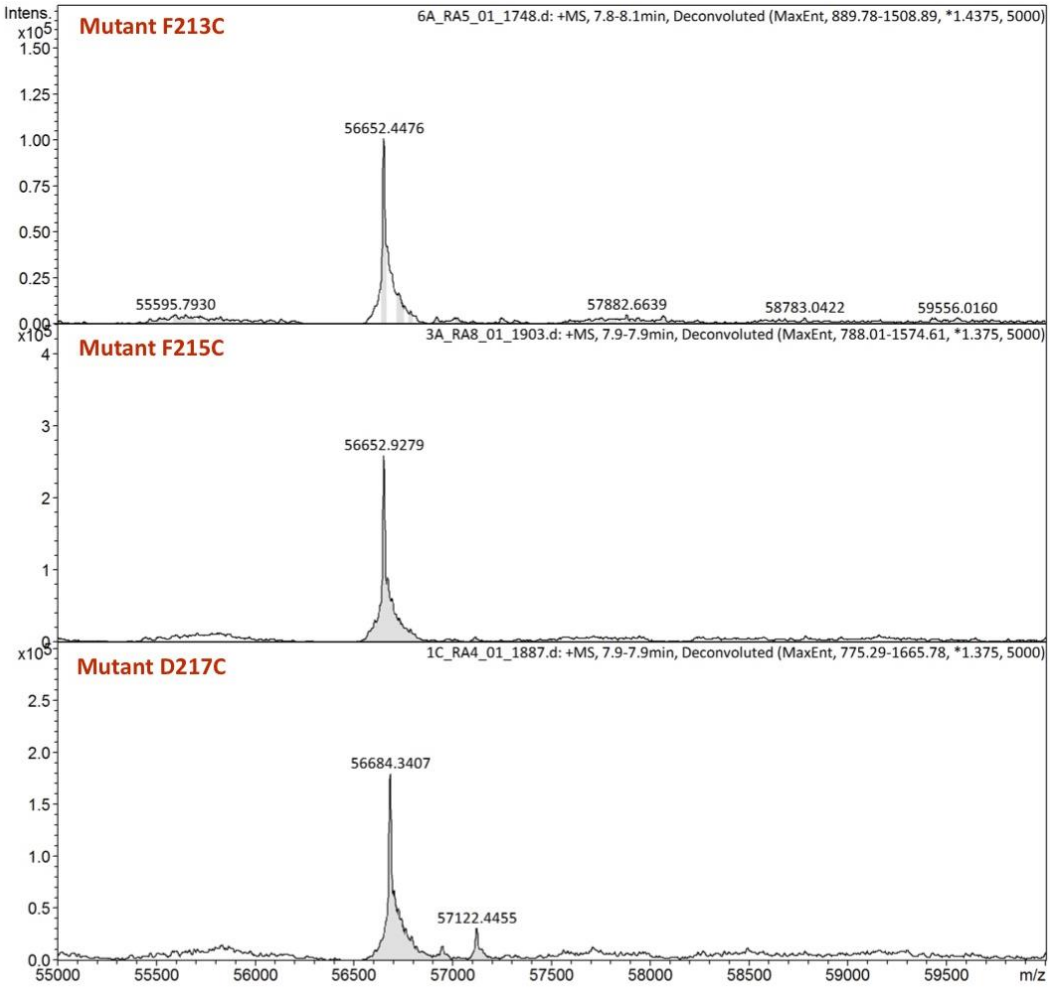

Enzyme	Theoretical Mass	Mass Found	Standard Deviation
Mutant F213C	56625.11	56652.48750	0.05643
Mutant F215C	56625.11	56652.81980	0.15288
Mutant D217C	56669.15	56684.70473	0.31595

6. COPPER CATALYZED AZIDE-ALKYNE CYCLOADDITION CONJUGATION RESULTS

The first site-selective bioconjugation method tested was the Schultz method for insertion of unnatural amino acids.[17] This elegant technique of incorporating unnatural amino has been applied to select P450s but not to CYP3A4.[18-20] Aiming to minimize changes to the site's electronic environment, we chose to replace existing phenylalanine residues at positions F213, F215 or F219 with *O*-propargyl tyrosine (OPgY), allowing for subsequent bioconjugation using the copper catalyzed azide-alkyne cyclization (CuAAC) (Figure S12A). Successful incorporation of the unnatural amino acid was confirmed using mass spectrometry (HPLC-MS-QToF) (Figure S13) yielding 1-3 mg/L of P450. Conjugation of an azide derivative of AlexaFluor488 to the mutant enzyme was achieved at 30ºC in 1 hour and confirmed *via* gel electrophoresis (SDS-PAGE) (Figures 12B). Unfortunately the conditions used for the bioconjugation reaction were found to be detrimental to enzyme activity (Figure S12C). Although no individual component of the CuAAC reaction mixture was entirely responsible for the loss of activity, the reaction components as an ensemble proved to be harmful to the enzyme.

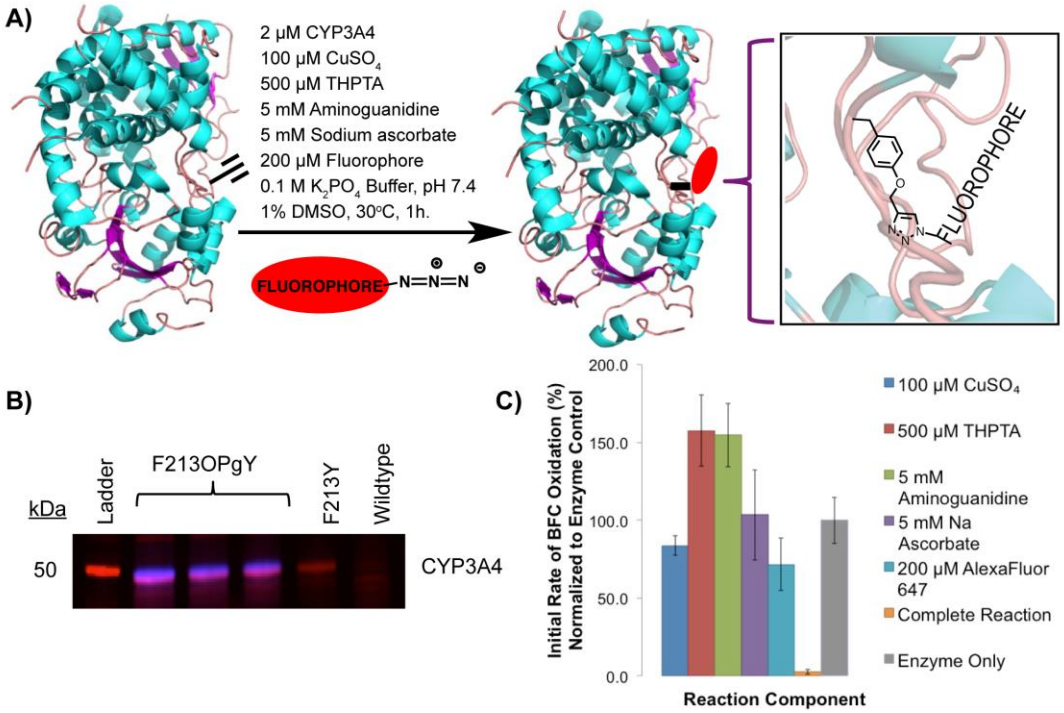

Figure S12. Copper catalyzed azide alkyne cyclization for bioconjugation to an *O*-propargyl tyrosine-containing CYP3A4 mutant. A) Reaction scheme showing reaction conditions for conjugation of the fluorophore to mutated CYP3A4. B) SDS-PAGE showing conjugation of AlexaFluor488 to the alkyne containing CYP3A4 mutant, compared with unlabeled mutant and wildtype enzyme. Unlabeled protein is shown by red bands, protein labeled by the fluorophore is shown by blue bands. C) The effect of each reaction component on the metabolism of BFC by unlabelled F213OPgY CYP3A4. Shown are the initial rates normalized to a control (enzyme only) showing the activity of the mutant enzyme before bioconjugation. The "complete reaction" control is lacking only the maleimide ligand. The initial rates are an average of measurements conducted in triplicate with the standard deviation shown by error bars.

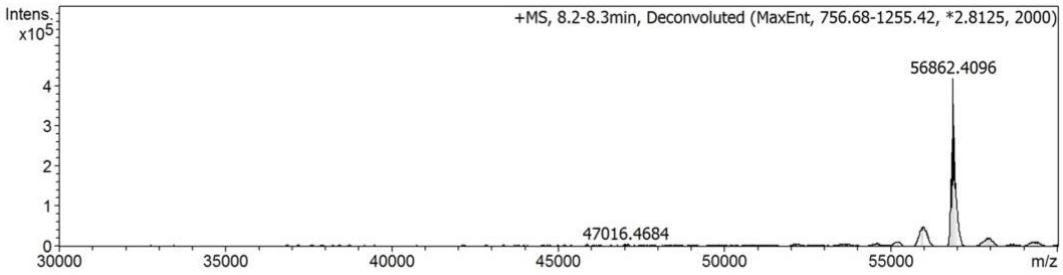

Enzyme	Theoretical Mass	Mass Found
F213OPgY	56835.45	56862.4096

Figure S13. Deconvoluted mass spectrum of *O*-propargyl tyrosine CYP3A4 mutant HPLC-MS-QTof was used to confirm the incorporation of the unnatural amino acid into the allosteric pocked of CYP3A4.

7. REFERENCES

(1) Tukey, J. W. (1949) Comparing individual means in the analysis of variance. *Biometrics 5*, 99-114.

(2) Isin, E. M., and Guengerich, F. P. (2006) Kinetics and Thermodynamics of Ligand Binding by Cytochrome P450 3A4. *J. Biol. Chem. 281*, 9127-9136.

(3) Das, A., Zhao, J., Schatz, G. C., Sligar, S. G., and Van Duyne, R. P. (2009) Screening of type I and II drug binding to human cytochrome P450-3A4 in nanodiscs by localized surface plasmon resonance spectroscopy. *Anal. Chem. 81*, 3754-3759.

(4) Trubetskoy, O. V., Gibson, J. R., and Marks, B. D. (2005) Highly miniaturized formats for in vitro drug metabolism assays using vivid fluorescent substrates and recombinant human cytochrome P450 enzymes. *J. Biomol. Screen. 10*, 56-66.

(5) Young, T. S., Ahmad, I., Yin, J. A., and Schultz, P. G. (2010) An enhanced system for unnatural amino acid mutagenesis in E. coli. *J. Mol. Biol. 395*, 361-374.

(6) Domanski, T. L., Liu, J., Harlow, G. R., and Halpert, J. R. (1998) Analysis of four residues within substrate recognition site 4 of human cytochrome P450 3A4: role in steroid hydroxylase activity and alpha-naphthoflavone stimulation. *Arch. Biochem. Biophys. 350*, 223-232.

(7) Tsalkova, T. N., Davydova, N. Y., Halpert, J. R., and Davydov, D. R. (2007) Mechanism of interactions of alpha-naphthoflavone with cytochrome P450 3A4 explored with an engineered enzyme bearing a fluorescent probe. *Biochemistry 46*, 106-119.

(8) Ménard, A., Huang, Y., Karam, P., Cosa, G., and Auclair, K. (2012) Site-Specific Fluorescent Labeling and Oriented Immobilization of a Triple Mutant of CYP3A4 via C64. *Bioconjugate Chem. 23*, 826-836.

(9) Omura, T., and Sato, R. (1964) The Carbon Monoxide-Binding Pigment of Liver Microsomes. II. Solubilization, Purification, and Properties. *J. Biol. Chem. 239*, 2379-2385.

(10) Chefson, A., Zhao, J., and Auclair, K. (2006) Replacement of natural cofactors by selected hydrogen peroxide donors or organic peroxides results in improved activity for CYP3A4 and CYP2D6. *Chembiochem 7*, 916-919.
(11) Krauser, J. A., Voehler, M., Tseng, L. H., Schefer, A. B., Godejohann, M., and Guengerich, F. P. (2004) Testosterone 1beta-hydroxylation by human cytochrome P450 3A4. *Eur. J. Biochem. 271*, 3962-3969.
(12) Córdoba, O. L., Linskens, S. B., Dacci, E., and Santomé, J. A. (1997) 'In gel' cleavage with cyanogen bromide for protein internal sequencing. *J. Biochem. Bioph. Methods 35*, 1-10.
(13) Haider, S. R., Reid, H. J., and Sharp, B. L. (2012) Tricine-SDS-PAGE. *Methods Mol. Biol. 869*, 81-91.
(14) Deiters, A., Cropp, T. A., Mukherji, M., Chin, J. W., Anderson, J. C., and Schultz, P. G. (2003) Adding amino acids with novel reactivity to the genetic code of Saccharomyces cerevisiae. *J. Am. Chem. Soc. 125*, 11782-11783.
(15) Zhang, Z., Yin, L., Xu, Y., Tong, R., Lu, Y., Ren, J., and Cheng, J. (2012) Facile functionalization of polyesters through thiol-yne chemistry for the design of degradable, cell-penetrating and gene delivery dual-functional agents. *Biomacromolecules 13*, 3456-3462.
(16) Dong, M. S., Bell, L. C., Guo, Z., Phillips, D. R., Blair, I. A., and Guengerich, F. P. (1996) Identification of retained N-formylmethionine in bacterial recombinant mammalian cytochrome P450 proteins with the N-terminal sequence MALLLAVFL...: roles of residues 3-5 in retention and membrane topology. *Biochemistry 35*, 10031-10040.
(17) Deiters, A., and Schultz, P. G. (2005) In vivo incorporation of an alkyne into proteins in Escherichia coli. *Bioorg. Med. Chem. Lett. 15*, 1521-1524.
(18) Basudhar, D., Madrona, Y., Kandel, S., Lampe, J. N., Nishida, C. R., and Ortiz de Montellano, P. R. (2015) Analysis of cytochrome P450 CYP119 ligand-dependent conformational dynamics by two-dimensional NMR and x-ray crystallography. *J. Biol. Chem. 290*, 10000-10017.
(19) Kolev, J. N., Zaengle, J. M., Ravikumar, R., and Fasan, R. (2014) Enhancing the efficiency and regioselectivity of P450 oxidation catalysts by unnatural amino acid mutagenesis. *ChemBioChem 15*, 1001-1010.
(20) Lampe, J. N., Brandman, R., Sivaramakrishnan, S., and Ortiz de Montellano, P. R. (2010) Two-dimensional NMR and all-atom molecular dynamics of cytochrome P450 CYP119 reveal hidden conformational substates. *J. Biol. Chem. 285*, 9594-9603.